

LIMIT BEHAVIOUR OF THE TRUNCATED PATHWISE FOURIER-TRANSFORMATION OF LÉVY-DRIVEN CARMA PROCESSES FOR NON-EQUIDISTANT DISCRETE TIME OBSERVATIONS

ŻYWILLA FECHNER ^{1,2} AND ROBERT STELZER ²

ABSTRACT. This paper considers a continuous time analogue of the classical autoregressive moving average processes, Lévy-driven CARMA processes. First we describe limiting properties of the periodogram by means of the so-called truncated Fourier transform if observations are available continuously. The obtained results are in accordance with their counterparts from the discrete-time case. Then we discuss the numerical approximation of the truncated Fourier transform based on non-equidistant high frequency data. In order to ensure convergence of the numerical approximation to the true value of the truncated Fourier transform a certain control on the maximal distance between observations and the number of observations is needed. We obtain both convergence to the continuous time quantity and asymptotic normality under a high-frequency infinite time horizon limit.

1. INTRODUCTION

The classical autoregressive moving average process ARMA has been broadly discussed in the literature. For a comprehensive discussion see e.g. the monograph by Brockwell and Davis [7] and references therein. In the discrete time models we restrict ourselves to observations at fixed equidistant points in time. In many cases these observations made at discrete times come from an underlying continuous process, thus the natural question arises: can we model also the time series in continuous time? One of the earliest results dealing with properties of such processes can be found in Doob [11]. Later this problem was discussed by Brockwell in [4] for continuous time ARMA processes driven by Gaussian noise. The next step was to extend these ideas to the models with noise modelled by jump processes, so-called Lévy-driven CARMA models introduced by Brockwell in [3]. In these papers time series are modelled as continuous time processes with continuous time noises (with or without jumps) and the inference is based mainly on discrete equidistant data. One of the latest results can be found in the paper [8] of Brockwell, Davis and Yang, which considers QML estimations of the AR and MA parameters based on equidistant observations.

The estimation procedure of Lévy-driven CARMA processes in high-frequency settings has been discussed by Fasen and Fuchs in [13], where the authors deal with the limit behaviour of the periodogram of CARMA processes under equidistant sampling when the sampling interval tends to 0. The results are analogous to ARMA processes: the periodogram for CARMA processes is not a consistent estimator of the spectral density function, but after appropriate smoothing the consistency can be obtained. Some related results were discussed by Fasen and Fuchs in [14], where asymptotic distributions of periodograms of

2010 *Mathematics Subject Classification.* Primary 62M10, 62M15, Secondary 60G10, 60G51 .

Key words and phrases. CARMA Process, Frequency Domain, High-frequency Data, Lévy Process, Trapezoidal Rule.

CARMA processes driven by a symmetric α -stable Lévy noise are obtained and where it is shown that the vector composed of periodograms for various frequencies converges in distribution to a function of a multidimensional stable random vector. Likewise, Fasen [12] considers the behaviour of the periodogram for an equidistantly sampled continuous time moving average process when only the number of observations goes to infinity.

The problem of statistical analysis of such processes has been studied further for example by Gillberg in his dissertation [15], where different approaches to the estimation of CARMA processes with Gaussian noise are discussed both using equidistant and non-equidistant observations. The author works mainly in the frequency domain. He describes the properties of the truncated Fourier transform of a CARMA process with Gaussian noise on a fixed interval $[0, T]$ based on equidistant frequencies. In the non-equidistant case he has used a method based on splines in order to find an approximation of the spectral density.

Another approach for the estimation of a zero-mean stationary process $(Y_t)_{t \in \mathbb{R}}$ with finite second-order moments and continuous covariance function has been discussed by Lii and Masry in [16] and [17], where they described some properties of a smoothed periodogram. Here observations are assumed to be given on a random grid (τ_k) of an interval $[0, T]$, where τ_k is a stationary point process on the real line which is independent of $(Y_t)_{t \in \mathbb{R}}$.

In the present paper we are going to describe the asymptotic behaviour of the so-called truncated Fourier transform of a CARMA process, which is a building block for an estimation of the spectral density of a CARMA process. We are going to use some of the ideas from [15] to prove results in more general settings.

The paper is structured as follows: first we recall second order Lévy-driven CARMA models and summarize the results needed later in Section 2. Then we define in Section 3 the truncated Fourier transform of a CARMA process and we investigate its asymptotic properties at a fixed frequency: for a non-zero frequency we obtain that the limiting law of the real and imaginary part is the two dimensional normal distribution with mean zero and the covariance matrix depending on the spectral density of the CARMA process. If we consider the truncated Fourier transform at zero, we obtain a one dimensional normal law with mean zero and variance depending only on two parameters of the CARMA process. We show that the limiting law of the joint distribution of the squared modulus of the truncated Fourier transform at different positive frequencies converges to a vector of independent and exponentially distributed random variables with mean depending on the values of the spectral density. All these results can be interpreted as the limiting behaviour of the truncated Fourier transform when the CARMA process is observed continuously. The next step in Section 3.2 is to approximate the truncated Fourier transform when the CARMA process is observed on a non-equidistant deterministic grid. In order to find a numerical approximation value of the truncated Fourier transform we apply the trapezoidal rule. We are interested in the convergence of the truncated Fourier transform when the length of the interval T goes to infinity and the mesh of the grid to zero. Since the interplay of the length of the interval, of the number of elements of the grid and of the maximal distance between the elements of the grid plays a crucial role, in order to ensure the convergence of the approximating sum to the true value of the truncated Fourier transform we have to impose some limiting conditions on these quantities. In the last Section 4 we look at some illustrative simulations of the truncated Fourier transform based on non-equidistant observations. We consider Ornstein-Uhlenbeck type (CAR(1)) and CARMA(2,1) processes driven by a standard Brownian motion, a Variance Gamma process and a “two-sided Poisson process” and we compare our simulations with the theoretical asymptotic distributions described earlier.

Notation. The symbol $\mathbb{N} := \{1, 2, 3, \dots\}$ denotes the set of positive integers, $\mathbb{N}_0 := \mathbb{N} \cup \{0\}$, \mathbb{R} is the set of real numbers and \mathbb{C} denotes the set of complex numbers. The symbol $\mathbb{R}^{m \times n}$, resp. $\mathbb{C}^{m \times n}$ denotes the space of real- (resp. complex-) valued matrices with m rows and n columns. For $A \in \mathbb{C}^{m \times n}$ the symbol A^T denotes the transposed of a matrix A . We are working on a given filtered probability space $(\Omega, \mathcal{F}, (\mathcal{F}_t)_{t \geq 0}, \mathbb{P})$ satisfying the usual hypothesis (cf. Protter [20], Chapter 1).

Moreover, by $X \stackrel{d}{=} Y$ we denote that the random variables X and Y are equal in distribution.

2. PRELIMINARIES

We begin with the model set-up given by Brockwell (see [3], [4]). A second-order Lévy-driven continuous-time ARMA(p, q) process is defined in terms of a state-space representation of the formal differential equation

$$(1) \quad a(D)Y(t) = b(D)DL(t), \quad t \geq 0.$$

Here, D denotes differentiation with respect to t , non-negative integers p, q satisfying $p > q$ and $(L(t))_{t \geq 0}$ is a one dimensional Lévy process (i.e. a continuous time process with stationary and independent increments and $L(0) = 0$ a.s.) with $\mathbb{E}L(1)^2 < \infty$. A comprehensive monograph dealing with Lévy processes is e.g. [1]. The polynomials

$$a(z) := z^p + a_1 z^{p-1} + \dots + a_p, \quad b(z) := b_0 + b_1 z + \dots + b_{p-1} z^{p-1},$$

are called the *autoregressive*- and *moving average* polynomial, respectively. We assume that $b_q \neq 0$ and $b_j = 0$ for $q < j < p$. The *state-space representation* consists of the *observation* and *state equations*:

$$(2) \quad Y(t) = \mathbf{b}^T \mathbf{X}(t),$$

$$(3) \quad d\mathbf{X}(t) = \mathbf{A}\mathbf{X}(t)dt + \mathbf{e}dL(t),$$

where

$$\mathbf{A} := \begin{bmatrix} 0 & 1 & 0 & \dots & 0 \\ 0 & 0 & 1 & \dots & 0 \\ \vdots & \vdots & \vdots & \ddots & \vdots \\ 0 & 0 & 0 & \dots & 1 \\ -a_p & -a_{p-1} & -a_{p-2} & \dots & -a_1 \end{bmatrix}, \quad \mathbf{X}(t) := \begin{bmatrix} X(t) \\ X^{(1)}(t) \\ \vdots \\ X^{(p-2)}(t) \\ X^{(p-1)}(t) \end{bmatrix},$$

$$\mathbf{e} := [0, \dots, 0, 1]^T, \quad \mathbf{b} := [b_0, b_1, \dots, b_{p-1}]^T,$$

i.e.

$$\mathbf{A} \in \mathbb{R}^{p \times p}, \quad \mathbf{X}(t) \in \mathbb{R}^{p \times 1} \quad \mathbf{e} \in \mathbb{R}^p, \quad \mathbf{b} \in \mathbb{R}^p.$$

If $p = 1$, we set $\mathbf{A} = -a_1$.

Assumption 2.1. *The Lévy process satisfies $\mathbb{E}L(1) = 0$ and $\mathbb{E}|L(1)|^2 = \sigma^2 < \infty$.*

Observe that $\mathbb{E}[L(s)L(t)] = \min\{s, t\}\mathbb{E}|L(1)|^2$. It was shown by Brockwell in [6] that the solution $\mathbf{X}(t)$ of (3) satisfies

$$(4) \quad \mathbf{X}(t) = e^{\mathbf{A}t} \mathbf{X}(0) + \int_0^t e^{\mathbf{A}(t-u)} \mathbf{e} dL(u),$$

where the integral is defined as the L^2 -limit of approximating Riemann sums.

Assumption 2.2. $\mathbf{X}(0)$ is independent of $(L(t))_{t \geq 0}$.

From now on let us assume that Assumption 2.2 holds. It is well-known ([6, Proposition 2]) that under Assumptions 2.1 and 2.2 the process $\{\mathbf{X}(t)\}_{t \geq 0}$ is strictly stationary and causal iff $\mathbf{X}(0)$ has the same distribution as $\int_0^\infty e^{\mathbf{A}u} \mathbf{e} dL(u)$ and the p (not necessarily distinct) eigenvalues $\lambda_1, \dots, \lambda_p$ of \mathbf{A} have negative real parts, i.e.

$$\Re(\lambda_i) < 0, \quad i = 1, \dots, p.$$

Now we extend the Lévy process $(L(u))_{u \geq 0}$ to the whole line in the usual way: Let $\tilde{L} = (\tilde{L}(t))_{t \geq 0}$ be an independent copy of $(L(t))_{t \geq 0}$. For $t \in \mathbb{R}$ we define

$$L^*(t) := L(t)\mathbf{1}_{[0, \infty)}(t) + \tilde{L}(-t-)\mathbf{1}_{(-\infty, 0]}(t).$$

In order to get stationary solutions of (3) we need the following assumptions:

Assumption 2.3. All eigenvalues of \mathbf{A} have strictly negative real parts.

Assumption 2.4.

$$\mathbf{X}(0) \stackrel{d}{=} \int_{-\infty}^0 e^{-\mathbf{A}u} \mathbf{e} dL^*(u)$$

In Brockwell [6] it was shown that if Assumptions 2.3 and 2.4 are satisfied the process $\{\mathbf{X}(t)\}_{t \in \mathbb{R}}$ given by

$$(5) \quad \mathbf{X}(t) = \int_{-\infty}^t e^{\mathbf{A}(t-u)} \mathbf{e} dL^*(u)$$

is a strictly stationary solution of (3) (with L replaced by L^*) for $t \in \mathbb{R}$ with corresponding CARMA process

$$(6) \quad Y(t) = \int_{-\infty}^t \mathbf{b}^T e^{\mathbf{A}(t-u)} \mathbf{e} dL^*(u).$$

For $t \geq 0$ one can rewrite it in the following form

$$(7) \quad Y(t) = \mathbf{b}^T e^{\mathbf{A}t} \mathbf{X}(0) + \int_0^t \mathbf{b}^T e^{\mathbf{A}(t-u)} \mathbf{e} dL(u).$$

In the present paper the spectral density of a CARMA process plays a crucial role. The spectral density is the Fourier transform of the autocovariance function $\gamma_Y(h) := \text{Cov}(Y(0), Y(h))$ for $h \in \mathbb{R}$. The spectral density of a CARMA process is

$$(8) \quad f_Y(\omega) = \frac{1}{2\pi} \int_{-\infty}^{\infty} \gamma_Y(h) e^{-ih\omega} dh = \frac{\sigma^2 |b(i\omega)|^2}{2\pi |a(i\omega)|^2}, \quad \omega \in \mathbb{R}.$$

3. LIMIT BEHAVIOUR OF THE FOURIER TRANSFORM

In this section we are going to deal with the Fourier transform of the CARMA process assuming that the observations are given continuously on the time interval $[0, T]$. A similar idea for Gaussian CARMA processes was presented in [15] for equidistant observations. The truncated continuous-time Fourier transform of the process Y at a fixed frequency $\omega \in \mathbb{R}$ is given by

$$\mathcal{F}_T(Y)(\omega) := \frac{1}{\sqrt{T}} \int_0^T Y(t) e^{-i\omega t} dt.$$

Observe that the norming constant $\frac{1}{\sqrt{T}}$ is taken as this ensures convergence in distribution for $T \rightarrow \infty$ as will be shown later.

3.1. Properties of the Truncated Fourier Transform of a CARMA Process. First we derive an alternative representation.

Lemma 3.1. *Let \mathbf{X} and Y be processes given by the state-space representation (2) and (3). Suppose that Assumptions 2.1, 2.2 and 2.3 are satisfied. Then the truncated Fourier transform of the CARMA process Y at a fixed frequency $\omega \in \mathbb{R}$ is of the form*

$$(9) \quad \mathcal{F}_T(Y)(\omega) = \frac{1}{\sqrt{T}} \frac{b(i\omega)}{a(i\omega)} \int_0^T e^{-i\omega t} dL(t) + \frac{1}{\sqrt{T}} \mathbf{b}^T (i\omega I - A)^{-1} (\mathbf{X}(0) - e^{-i\omega T} \mathbf{X}(T)),$$

or equivalently

$$(10) \quad \mathcal{F}_T(Y)(\omega) = \frac{1}{\sqrt{T}} \mathbf{b}^T (i\omega I - A)^{-1} \times \left[\int_0^T \left(e^{-i\omega u} - e^{-i\omega T} e^{\mathbf{A}(T-u)} \right) \mathbf{e} dL(u) + \left(I - e^{(-i\omega I + \mathbf{A})T} \right) \mathbf{X}(0) \right].$$

PROOF. Let ω be an arbitrary frequency. Observe that by Corollary 3.4 from [21, p. 51] one has

$$\mathbf{b}^T (\mathbf{A} - i\omega I)^{-1} \mathbf{e} = -\frac{b(i\omega)}{a(i\omega)}.$$

Denote

$$F(t) = \mathbf{b}^T (\mathbf{A} - i\omega I)^{-1} e^{(\mathbf{A} - i\omega I)t}, \quad t \in [0, T],$$

$$G(t) = \int_0^t e^{-\mathbf{A}u} \mathbf{e} dL(u) \quad t \in [0, T].$$

Observe that $G(0) = 0$ and since F is continuous and of finite variation, we get $[F, G] = 0$, where $[\cdot, \cdot]$ denotes the usual quadratic covariation of semimartingales (see e.g. [20]). Applying the (multidimensional) integration by parts formula

$$\begin{aligned} \int_0^T dF(t)G(t) &= F(T)G(T) - F(0)G(0) - \int_0^T F(t)dG(t) - [F, G] \\ &= F(T)G(T) - \int_0^T F(t)dG(t) \end{aligned}$$

we obtain

$$\begin{aligned} \int_0^T dF(t)G(t) &= \int_0^T \mathbf{b}^T (\mathbf{A} - i\omega I)^{-1} (\mathbf{A} - i\omega I) e^{(\mathbf{A} - i\omega I)t} \int_0^t e^{-\mathbf{A}u} \mathbf{e} dL(u) dt \\ &= \int_0^T \int_0^t \mathbf{b}^T e^{\mathbf{A}(t-u)} \mathbf{e} dL(u) e^{-i\omega t} dt \\ &= \mathbf{b}^T (\mathbf{A} - i\omega I)^{-1} e^{(\mathbf{A} - i\omega I)T} \int_0^T e^{-\mathbf{A}t} \mathbf{e} dL(t) - \int_0^T \mathbf{b}^T (\mathbf{A} - i\omega I)^{-1} e^{(\mathbf{A} - i\omega I)t} e^{-\mathbf{A}t} \mathbf{e} dL(t) \\ &= \mathbf{b}^T (\mathbf{A} - i\omega I)^{-1} e^{-i\omega T} \int_0^T e^{\mathbf{A}(T-t)} \mathbf{e} dL(t) + \frac{b(i\omega)}{a(i\omega)} \int_0^T e^{-i\omega t} dL(t). \end{aligned}$$

Thus

$$(11) \quad \begin{aligned} &\int_0^T \int_0^t \mathbf{b}^T e^{\mathbf{A}(t-u)} \mathbf{e} dL(u) e^{-i\omega t} dt \\ &= \mathbf{b}^T (\mathbf{A} - i\omega I)^{-1} e^{-i\omega T} \int_0^T e^{\mathbf{A}(T-t)} \mathbf{e} dL(t) + \frac{b(i\omega)}{a(i\omega)} \int_0^T e^{-i\omega t} dL(t). \end{aligned}$$

Using the form of the strictly stationary solution of (3) given in (4) we get

$$(12) \quad \int_0^T e^{\mathbf{A}(T-t)} \mathbf{e} dL(t) = \mathbf{X}(T) - e^{\mathbf{A}T} \mathbf{X}(0).$$

Moreover, since $\int_0^T e^{(\mathbf{A}-i\omega I)t} dt = (i\omega I - \mathbf{A})^{-1} (I - e^{(\mathbf{A}-i\omega I)T})$, we have

$$(13) \quad \int_0^T \mathbf{b}^T e^{(\mathbf{A}-i\omega I)t} \mathbf{X}(0) dt = \mathbf{b}^T (i\omega I - \mathbf{A})^{-1} (I - e^{(\mathbf{A}-i\omega I)T}) \mathbf{X}(0).$$

We have

$$\begin{aligned} \mathcal{F}_T(Y)(\omega) &= \frac{1}{\sqrt{T}} \int_0^T Y(t) e^{-i\omega t} dt \\ &\stackrel{(7)}{=} \frac{1}{\sqrt{T}} \int_0^T \left(\mathbf{b}^T e^{\mathbf{A}t} \mathbf{X}(0) + \int_0^t \mathbf{b}^T e^{\mathbf{A}(t-u)} \mathbf{e} dL(u) \right) e^{-i\omega t} dt \\ &\stackrel{(11), (12), (13)}{=} \frac{1}{\sqrt{T}} \frac{b(i\omega)}{a(i\omega)} \int_0^T e^{-i\omega u} dL(u) + \frac{1}{\sqrt{T}} \mathbf{b}^T (i\omega I - \mathbf{A})^{-1} (\mathbf{X}(0) - e^{-i\omega T} \mathbf{X}(T)). \end{aligned}$$

To get the equivalent form note,

$$\begin{aligned} \sqrt{T} \mathcal{F}(Y)(\omega) &= \mathbf{b}^T (i\omega I - \mathbf{A})^{-1} \left[\mathbf{e} \int_0^T e^{-i\omega u} dL(u) + (\mathbf{X}(0) - e^{-i\omega T} \mathbf{X}(T)) \right] \\ &\stackrel{(12)}{=} \mathbf{b}^T (i\omega I - \mathbf{A})^{-1} \left[\int_0^T \left(e^{-i\omega u} - e^{-i\omega T} e^{\mathbf{A}(T-u)} \right) \mathbf{e} dL(u) + \left(I - e^{(-i\omega I + \mathbf{A})T} \right) \mathbf{X}(0) \right], \end{aligned}$$

which completes the proof of this Lemma. \square

The next step is to calculate moments of the truncated Fourier transform. First, recall the so-called *compensation formula*: If $(L_t)_{t \geq 0}$ is a Lévy process with finite first moments and f is a bounded deterministic function, then

$$(14) \quad \mathbb{E} \left[\int_0^T f(u) dL_u \right] = \mathbb{E}[L_1] \int_0^T f(s) ds.$$

Secondly, observe that the solution of the system (2) and (3) is of the form (4), where \mathbf{X} is the process with mean $m(t) = \mathbb{E}[\mathbf{X}(t)]$ and $P_X(t) = \mathbb{E}[\mathbf{X}(t)\mathbf{X}(t)^T]$ satisfying

$$\begin{aligned} m_X(t) &= e^{\mathbf{A}t} m_X(0) \\ (15) \quad P_X(t) &= e^{\mathbf{A}t} P_X(0) e^{\mathbf{A}^T t} + \sigma^2 \int_0^t e^{\mathbf{A}(t-u)} \mathbf{e} \mathbf{e}^T e^{\mathbf{A}^T(t-u)} du \end{aligned}$$

In particular, for stationary processes these solutions are constant and the so called Lyapunov equation

$$(16) \quad \mathbf{A} P_X + P_X \mathbf{A}^T + \sigma^2 \mathbf{e} \mathbf{e}^T = 0$$

holds true. For Lévy-driven CARMA processes the form of the autocovariance function in terms of solutions of Lyapunov equations is formulated e.g. in [19, Proposition 3.13.].

We are first going to show that the truncated Fourier transform of a stationary CARMA process is a zero-mean random variable. Next, we find the covariance between the truncated Fourier transform at two different frequencies. As we have mentioned earlier, the spectral density function plays a central role.

Theorem 3.2. *Let \mathbf{X} and Y be processes given by the state-space representation (2) and (3). Suppose that Assumptions 2.1, 2.2, 2.3 and 2.4 are satisfied. Then $\mathbb{E}(\mathcal{F}_T(Y)(\omega)) = 0$ for all $\omega \in \mathbb{R}$. For $\omega_1, \omega_2 \in \mathbb{R}$ we have*

$$(17) \quad \mathbb{E}[\mathcal{F}_T(Y)(\omega_1)\mathcal{F}_T(Y)(\omega_2)] = \sigma^2 \frac{|b(i\omega_1)|^2}{|a(i\omega_1)|^2} + \frac{1}{T}K(T, \omega_1, -\omega_1), \quad \text{if } \omega_1 = -\omega_2$$

and

$$(18) \quad \mathbb{E}[\mathcal{F}_T(Y)(\omega_1)\mathcal{F}_T(Y)(\omega_2)] = \frac{1}{T}K_1(T, \omega_1, \omega_2), \quad \text{if } \omega_1 \neq -\omega_2,$$

where K is a bounded function of T given by (20) below and

$$K_1(T, \omega_1, \omega_2) = K(T, \omega_1, \omega_2) + \mathbf{b}^T(i\omega_1 I - \mathbf{A})^{-1} \sigma^2 \frac{1 - \exp(-Ti(\omega_1 + \omega_2))}{i(\omega_1 + \omega_2)} \mathbf{e}\mathbf{e}^T(i\omega_2 I - \mathbf{A}^T)^{-1} \mathbf{b}.$$

PROOF. For the first part it is enough to observe that by the compensation formula $\mathbb{E}\left(\int_0^T e^{-i\omega u} dL(u)\right) = 0$ and $\mathbb{E}[\mathbf{X}(t)] = 0$. For the second part observe that using Lemma 3.1 and formula (10) we have

$$\begin{aligned} \mathbb{E}[\mathcal{F}_T(Y)(\omega_1)\mathcal{F}_T(Y)(\omega_2)] &= \frac{1}{T} \mathbf{b}^T(i\omega_1 I - \mathbf{A})^{-1} \times \\ &\mathbb{E}\left[\left(\int_0^T \left(e^{-i\omega_1 u} - e^{-i\omega_1 T} e^{\mathbf{A}(T-u)}\right) \mathbf{e} dL(u) + \left(I - e^{(-i\omega_1 I + \mathbf{A})T}\right) \mathbf{X}(0)\right) \times \right. \\ &\left.\left(\int_0^T \mathbf{e}^T \left(e^{-i\omega_2 u} - e^{-i\omega_2 T} e^{\mathbf{A}^T(T-u)}\right) dL(u) + \mathbf{X}(0)^T \left(I - e^{(-i\omega_2 I + \mathbf{A}^T)T}\right)\right)\right] \times \\ &(i\omega_2 I - \mathbf{A}^T)^{-1} \mathbf{b} = \frac{1}{T} \mathbf{b}^T(i\omega_1 I - \mathbf{A})^{-1} \tilde{I}(i\omega_2 I - \mathbf{A}^T)^{-1} \mathbf{b}, \end{aligned}$$

where $\tilde{I} = I_1 + I_2 + I_3 + I_4$ with

$$\begin{aligned} I_1 &:= \mathbb{E}\left[\int_0^T \left(e^{-i\omega_1 u} - e^{-i\omega_1 T} e^{\mathbf{A}(T-u)}\right) \mathbf{e} dL(u) \cdot \int_0^T \mathbf{e}^T \left(e^{-i\omega_2 u} - e^{-i\omega_2 T} e^{\mathbf{A}^T(T-u)}\right) dL(u)\right] \\ I_2 &:= \mathbb{E}\left[\int_0^T \left(e^{-i\omega_1 u} - e^{-i\omega_1 T} e^{\mathbf{A}(T-u)}\right) \mathbf{e} dL(u) \cdot \mathbf{X}(0)^T \left(I - e^{(-i\omega_2 I + \mathbf{A}^T)T}\right)\right] \\ I_3 &:= \mathbb{E}\left[\left(I - e^{(-i\omega_1 I + \mathbf{A})T}\right) \mathbf{X}(0) \cdot \int_0^T \mathbf{e}^T \left(e^{-i\omega_2 u} - e^{-i\omega_2 T} e^{\mathbf{A}^T(T-u)}\right) dL(u)\right] \\ I_4 &:= \mathbb{E}\left[\left(I - e^{(-i\omega_1 I + \mathbf{A})T}\right) \mathbf{X}(0) \mathbf{X}(0)^T \left(I - e^{(-i\omega_2 I + \mathbf{A}^T)T}\right)\right]. \end{aligned}$$

We have that $I_2 = I_3 = 0$ since $(L_t)_{t \geq 0}$ is independent of $\mathbf{X}(0)$. Observe that by the Itô isometry, the compensation formula and the fact that $\mathbb{E}[[L, L]_1] = \text{Var}(L(1)) = \sigma^2$ we have

$$\begin{aligned} I_1^1 &:= \mathbb{E}\left[\int_0^T e^{-i\omega_1 u} \mathbf{e} dL(u) \int_0^T \mathbf{e}^T e^{-i\omega_2 u} dL(u)\right] = \mathbb{E}\left[\int_0^T e^{-i(\omega_1 + \omega_2)u} \mathbf{e}\mathbf{e}^T d[L, L]_u\right] \\ &= \mathbb{E}[[L, L]_1] \int_0^T e^{-i(\omega_1 + \omega_2)u} \mathbf{e}\mathbf{e}^T du = \sigma^2 \int_0^T e^{-i(\omega_1 + \omega_2)u} \mathbf{e}\mathbf{e}^T du. \end{aligned}$$

Thus

$$(19) \quad I_1^1 = \begin{cases} \sigma^2 T \mathbf{e}\mathbf{e}^T, & \omega_1 = -\omega_2, \\ \sigma^2 \frac{1 - \exp(-Ti(\omega_1 + \omega_2))}{i(\omega_1 + \omega_2)} \mathbf{e}\mathbf{e}^T, & \omega_1 \neq -\omega_2. \end{cases}$$

Thus, if $\omega_1 = -\omega_2$, then

$$\frac{1}{T} \mathbf{b}^T(i\omega_1 I - \mathbf{A})^{-1} I_1^1(i\omega_2 I - \mathbf{A}^T)^{-1} \mathbf{b} = \frac{1}{T} \cdot \sigma^2 T \mathbf{b}^T(i\omega_1 I - \mathbf{A})^{-1} \mathbf{e}\mathbf{e}^T(i\omega_2 I - \mathbf{A}^T)^{-1} \mathbf{b}$$

$$\begin{aligned}
&= \sigma^2 \mathbf{b}^T (\mathbf{A} - i\omega_1 I)^{-1} \mathbf{e} \mathbf{e}^T (i\omega_1 I + \mathbf{A}^T)^{-1} \mathbf{b} \\
&= \sigma^2 \left(-\frac{b(i\omega_1)}{a(i\omega_1)} \right) \left(-\frac{b(-i\omega_1)}{a(-i\omega_1)} \right) = \sigma^2 \frac{|b(i\omega_1)|^2}{|a(i\omega_1)|^2}.
\end{aligned}$$

Now

$$\begin{aligned}
I_1^2 &:= \mathbb{E} \left[\int_0^T e^{-i\omega_1 u} \mathbf{e} dL(u) \int_0^T \mathbf{e}^T e^{-i\omega_2 T} e^{\mathbf{A}^T(T-u)} dL(u) \right] \\
&= e^{-i\omega_2 T} \mathbb{E} \left[\int_0^T e^{-i\omega_1 u} \mathbf{e} \mathbf{e}^T e^{\mathbf{A}^T(T-u)} d[L, L]_u \right] \\
&= e^{-i\omega_2 T} \mathbb{E}[[L, L]_1] \int_0^T e^{-i\omega_1 u} \mathbf{e} \mathbf{e}^T e^{\mathbf{A}^T(T-u)} du \\
&= e^{-i\omega_2 T} \sigma^2 \int_0^T e^{-i\omega_1 u} \mathbf{e} \mathbf{e}^T e^{\mathbf{A}^T(T-u)} du.
\end{aligned}$$

In the same way

$$\begin{aligned}
I_1^3 &:= \mathbb{E} \left[\int_0^T e^{-i\omega_1 T} e^{\mathbf{A}(T-u)} \mathbf{e} dL(u) \int_0^T \mathbf{e}^T e^{-i\omega_2 u} dL(u) \right] \\
&= e^{-i\omega_1 T} \sigma^2 \int_0^T e^{\mathbf{A}(T-u)} \mathbf{e} \mathbf{e}^T e^{-i\omega_2 u} du.
\end{aligned}$$

Combining these two we arrive at

$$\begin{aligned}
I_1^2 + I_1^3 &= e^{-i(\omega_1 + \omega_2)T} \sigma^2 \left[\mathbf{e} \mathbf{e}^T (i\omega_1 I + \mathbf{A}^T)^{-1} \left(e^{(i\omega_1 I + \mathbf{A}^T)T} - I \right) \right. \\
&\quad \left. + (i\omega_2 I + \mathbf{A})^{-1} \left(e^{(i\omega_2 I + \mathbf{A})T} - I \right) \mathbf{e} \mathbf{e}^T \right].
\end{aligned}$$

Now

$$\begin{aligned}
I_1^4 &:= \mathbb{E} \left[\int_0^T e^{-i\omega_1 T} e^{\mathbf{A}(T-u)} \mathbf{e} dL(u) \int_0^T \mathbf{e}^T e^{-i\omega_2 T} e^{\mathbf{A}^T(T-u)} dL(u) \right] \\
&= e^{-i(\omega_1 + \omega_2)T} \sigma^2 \int_0^T e^{\mathbf{A}(T-u)} \mathbf{e} \mathbf{e}^T e^{\mathbf{A}^T(T-u)} du.
\end{aligned}$$

Now

$$\begin{aligned}
I_4 &= \mathbb{E}[\mathbf{X}(0)\mathbf{X}(0)^T] - e^{-i\omega_1 T} e^{\mathbf{A}T} \mathbb{E}[\mathbf{X}(0)\mathbf{X}(0)^T] - e^{-i\omega_2 T} \mathbb{E}[\mathbf{X}(0)\mathbf{X}(0)^T] e^{\mathbf{A}^T T} \\
&\quad + e^{-i(\omega_1 + \omega_2)T} e^{\mathbf{A}T} \mathbb{E}[\mathbf{X}(0)\mathbf{X}(0)^T] e^{\mathbf{A}^T T}.
\end{aligned}$$

By stationarity we have

$$\mathbb{E}[\mathbf{X}(0)\mathbf{X}(0)^T] =: P_X = P_X(0) = P_X(T),$$

where P_X satisfies (16). Combining this with (15) we obtain

$$\begin{aligned}
I_1^4 + I_4 &= P_X - e^{-i\omega_1 T} e^{\mathbf{A}T} P_X - e^{-i\omega_2 T} P_X e^{\mathbf{A}^T T} + e^{-i(\omega_1 + \omega_2)T} e^{\mathbf{A}T} P_X e^{\mathbf{A}^T T} \\
&\quad + e^{-i(\omega_1 + \omega_2)T} (P_X - e^{\mathbf{A}T} P_X e^{\mathbf{A}^T T}) \\
&= e^{-i\omega_1 T} P_X (I - e^{\mathbf{A}T}) + e^{-i\omega_2 T} (I - e^{\mathbf{A}^T}) P_X \\
&\quad + P_X (1 - e^{-i\omega_1 T} - e^{-i\omega_2 T} + e^{-i(\omega_1 + \omega_2)T}).
\end{aligned}$$

Since \mathbf{A} is a stable matrix, $e^{\mathbf{A}T}$ is bounded.

Thus

$$\begin{aligned}
(20) \quad K(T, \omega_1, \omega_2) = & \mathbf{b}^T (i\omega_1 I - \mathbf{A})^{-1} \left[e^{-i(\omega_1 + \omega_2)T} \sigma^2 \left[\mathbf{e} \mathbf{e}^T (i\omega_1 I + \mathbf{A}^T)^{-1} \left(e^{(i\omega_1 I + \mathbf{A}^T)T} - I \right) \right. \right. \\
& + (i\omega_2 I + \mathbf{A})^{-1} \left(e^{(i\omega_2 I + \mathbf{A})T} - I \right) \mathbf{e} \mathbf{e}^T \Big] \\
& + e^{-i\omega_1 T} P_X \left(I - e^{\mathbf{A}^T T} \right) + e^{-i\omega_2 T} \left(I - e^{\mathbf{A} T} \right) P_X \\
& \left. + P_X \left(1 - e^{-i\omega_1 T} - e^{-i\omega_2 T} + e^{-i(\omega_1 + \omega_2)T} \right) \right] (i\omega_2 I - \mathbf{A}^T)^{-1} \mathbf{b}
\end{aligned}$$

is bounded in T for fixed $\omega_1, \omega_2 \in \mathbb{R}$. \square

Now we give the form of the covariance matrix. Put

$$\Sigma(\omega_1, \omega_2) := [\Sigma_{ij}]_{1 \leq i, j \leq 4} = \mathbb{E} \left[\begin{bmatrix} \Re \mathcal{F}_T(Y)(\omega_1) \\ \Im \mathcal{F}_T(Y)(\omega_1) \\ \Re \mathcal{F}_T(Y)(\omega_2) \\ \Im \mathcal{F}_T(Y)(\omega_2) \end{bmatrix} \begin{bmatrix} \Re \mathcal{F}_T(Y)(\omega_1) \\ \Im \mathcal{F}_T(Y)(\omega_1) \\ \Re \mathcal{F}_T(Y)(\omega_2) \\ \Im \mathcal{F}_T(Y)(\omega_2) \end{bmatrix}^T \right].$$

Theorem 3.3. *Let \mathbf{X} and Y be processes given by the state-space representation (2) and (3). Suppose that Assumptions 2.1, 2.2, 2.3 and 2.4 are satisfied. For $\omega_1 \neq \omega_2$ and $\omega_1 \neq -\omega_2$ there exists a bounded matrix $K_2 \in \mathbb{C}^{4 \times 4}$ such that*

$$\Sigma(\omega_1, \omega_2) = \frac{1}{2} \sigma^2 \text{diag} \left(\frac{|b(i\omega_1)|^2}{|a(i\omega_1)|^2}, \frac{|b(i\omega_1)|^2}{|a(i\omega_1)|^2}, \frac{|b(i\omega_2)|^2}{|a(i\omega_2)|^2}, \frac{|b(i\omega_2)|^2}{|a(i\omega_2)|^2} \right) + \frac{1}{T} K_2.$$

Proof. For $k, l = 1, 2$ let us denote

$$\begin{aligned}
\Sigma_1(\omega_1, \omega_2) &:= \mathbb{E} [\Re \mathcal{F}_T(Y)(\omega_1) \Re \mathcal{F}_T(Y)(\omega_2)], \quad \Sigma_2(\omega_1, \omega_2) := \mathbb{E} [\Im \mathcal{F}_T(Y)(\omega_1) \Im \mathcal{F}_T(Y)(\omega_2)], \\
\Sigma_3(\omega_1, \omega_2) &:= \mathbb{E} [\Re \mathcal{F}_T(Y)(\omega_1) \Im \mathcal{F}_T(Y)(\omega_2)].
\end{aligned}$$

All entries $\Sigma_{i,j}$ of the matrix Σ are of one of the above forms. Indeed, Σ_{11}, Σ_{33} are of the form Σ_1 for $k = l$ and $k, l \in \{1, 2\}$. Similarly, Σ_{22}, Σ_{44} are of the form Σ_2 for $k = l$ and $k, l \in \{1, 2\}$. Moreover, Σ_{13}, Σ_{31} are of the form Σ_1 for $k \neq l$ and $k, l \in \{1, 2\}$ and Σ_{24}, Σ_{42} are of the form Σ_2 for $k \neq l$ and $k, l \in \{1, 2\}$. All other elements are of the form Σ_3 .

Observe that for each ω we have

$$\Re \mathcal{F}_T(Y)(\omega) = \frac{\mathcal{F}_T(Y)(\omega) + \mathcal{F}_T(Y)(-\omega)}{2}, \quad \Im \mathcal{F}_T(Y)(\omega) = \frac{\mathcal{F}_T(Y)(\omega) - \mathcal{F}_T(Y)(-\omega)}{2i}.$$

Using Theorem 3.2 we obtain

$$\begin{aligned}
\Sigma_1(\omega_1, \omega_2) &:= \begin{cases} \sigma^2 \frac{|b(0)|^2}{|a(0)|^2} + \frac{1}{T} K(0), & \omega_1 = \omega_2 = 0; \\ \frac{1}{2} \sigma^2 \frac{|b(i\omega_1)|^2}{|a(i\omega_1)|^2} + \frac{1}{T} K_{1,1}(\omega_1), & \omega_1 = \omega_2; \\ \frac{1}{2} \sigma^2 \frac{|b(i\omega_1)|^2}{|a(i\omega_1)|^2} + \frac{1}{T} K_{1,2}(\omega_1), & \omega_1 = -\omega_2; \\ \frac{1}{T} K_{1,3}(\omega_1, \omega_2), & \omega_1 \neq \omega_2 \text{ and } \omega_1 \neq -\omega_2, \end{cases} \\
\Sigma_2(\omega_1, \omega_2) &:= \begin{cases} 0, & \omega_1 = 0 \text{ or } \omega_2 = 0; \\ \frac{1}{2} \sigma^2 \frac{|b(i\omega_1)|^2}{|a(i\omega_1)|^2} + \frac{1}{T} K_{2,1}(\omega_1), & \omega_1 = \omega_2; \\ -\frac{1}{2} \sigma^2 \frac{|b(i\omega_1)|^2}{|a(i\omega_1)|^2} - \frac{1}{T} K_{2,2}(\omega_1), & \omega_1 = -\omega_2; \\ \frac{1}{T} K_{2,3}(\omega_1, \omega_2), & \omega_1 \neq \omega_2 \text{ and } \omega_1 \neq -\omega_2, \end{cases} \\
\Sigma_3(\omega_1, \omega_2) &:= \begin{cases} 0, & \omega_2 = 0; \\ \frac{1}{T} K_{3,1}(\omega_1), & \omega_1 = \omega_2 \text{ or } \omega_1 = -\omega_2; \\ \frac{1}{T} K_{3,2}(\omega_1, \omega_2), & \omega_1 \neq \omega_2 \text{ and } \omega_1 \neq -\omega_2. \end{cases}
\end{aligned}$$

Here K is given by (20) and $K_{i,j}$ are bounded in T for $i, j = 1, 2, 3$. \square

Now we are going to investigate asymptotic properties of the truncated Fourier transform. First, we will show that the second summand of (9) converges in probability to zero.

Lemma 3.4. *Let \mathbf{X} and Y be processes given by the state-space representation (2) and (3). Suppose that Assumptions 2.1, 2.2 and 2.3 are satisfied. Let*

$$\tilde{Z}(T) := \mathcal{F}_T(Y)(\omega) - \frac{1}{\sqrt{T}} \frac{b(i\omega)}{a(i\omega)} \int_0^T e^{-i\omega t} dL(t).$$

Then

$$\mathbb{P} - \lim_{T \rightarrow \infty} |\tilde{Z}(T)| = 0.$$

Proof. Observe that

$$\begin{aligned} |\tilde{Z}(T)| &= \left| \frac{1}{\sqrt{T}} \mathbf{b}^T (i\omega I - A)^{-1} [\mathbf{X}(0) - e^{-i\omega T} \mathbf{X}(T)] \right| \\ &\leq \frac{1}{\sqrt{T}} |\mathbf{b}^T (i\omega I - A)^{-1} \mathbf{X}(0)| + \frac{1}{\sqrt{T}} |\mathbf{b}^T (i\omega I - A)^{-1} \mathbf{X}(T)|. \end{aligned}$$

Obviously,

$$\lim_{T \rightarrow \infty} \frac{1}{\sqrt{T}} |\mathbf{b}^T (i\omega I - A)^{-1} \mathbf{X}(0)| = 0 \quad \text{a.s. as } T \rightarrow \infty.$$

Because of stationarity, $\mathbf{X}(T)$ is bounded in probability and $\frac{1}{\sqrt{T}}$ converges to zero thus

$$\frac{1}{\sqrt{T}} |\mathbf{b}^T (i\omega I - A)^{-1} \mathbf{X}(T)| \rightarrow 0 \text{ in probability.}$$

Therefore

$$\mathbb{P} - \lim_{T \rightarrow \infty} |\tilde{Z}(T)| = 0.$$

This completes the proof. \square

Now we will show that the first summand of formula (9) converges in distribution. Thus, together with Lemma 3.4 we obtain the limit in distribution of the truncated Fourier transform. We have two cases: the first case is if the frequency $\omega = 0$. Then the truncated Fourier transform is a real valued function. In the second case for frequencies $\omega \neq 0$ the truncated Fourier transform is a complex valued function. In both cases we first give the description of the distribution of the truncated Fourier transform and afterwards we describe the distribution of the squared modulus of the truncated Fourier transform.

Theorem 3.5. *Let \mathbf{X} and Y be processes given by the state-space representation (2) and (3). Suppose that Assumptions 2.1 and 2.3 are satisfied. Let*

$$Z(T) := \frac{1}{\sqrt{T}} \frac{b(0)}{a(0)} \int_0^T dL(t).$$

Then

$$d - \lim_{T \rightarrow \infty} Z(T) \sim \mathcal{N} \left(0, \left(\frac{b(0)}{a(0)} \right)^2 \sigma^2 \right), \quad d - \lim_{T \rightarrow \infty} \frac{1}{\sigma^2} \left| \frac{a(0)Z(T)}{b(0)} \right|^2 \sim \chi^2(1)$$

Proof. Observe that $\int_0^T dL(t) = L(T)$, thus $Z(T) = \frac{1}{\sqrt{T}} \frac{b(0)}{a(0)} L(T)$. By the standard Central Limit Theorem $d - \lim_{T \rightarrow \infty} \frac{1}{\sqrt{T}} L(T) = \mathcal{N}(0, \sigma^2)$. Therefore $d - \lim_{T \rightarrow \infty} \frac{1}{\sqrt{T}} \frac{b(0)}{a(0)} L(T) = \mathcal{N} \left(0, \left(\frac{b(0)}{a(0)} \right)^2 \sigma^2 \right)$.

Observe that for all $n \in \mathbb{N}$ the random variable $\frac{a(0)Z(n)}{b(0)\sigma} \sim \mathcal{N}(0, 1)$. Then by the continuous mapping theorem we have $d - \lim_{T \rightarrow \infty} \frac{1}{\sigma^2} \left| \frac{a(0)Z(T)}{b(0)} \right|^2 \sim \chi^2(1)$. \square

In order to find the asymptotic distribution of the truncated Fourier transform we use the multivariate Central Limit Theorem. Note that we state all results for positive frequencies as the corresponding results for negative can be obtained by taking the complex conjugate.

Theorem 3.6. *Let \mathbf{X} and Y be processes given by the state-space representation (2) and (3). Suppose that Assumptions 2.1 and 2.3 are satisfied. Assume that $\omega > 0$. Put*

$$Z(T) := \frac{1}{\sqrt{T}} \frac{b(i\omega)}{a(i\omega)} \int_0^T e^{-i\omega t} dL(t)$$

and

$$Z(T) = \begin{bmatrix} \Re Z(T) \\ \Im Z(T) \end{bmatrix}.$$

Then

$$d - \lim_{T \rightarrow \infty} Z(T) \sim \mathcal{N}(0, \Sigma),$$

$$\text{where } \Sigma = \frac{\sigma^2}{2} \left| \frac{b(i\omega)}{a(i\omega)} \right|^2 I_{2 \times 2}.$$

Proof. We first show that $\frac{1}{\sqrt{N}} \int_0^{\frac{2\pi N}{\omega}} e^{-i\omega t} dL(t)$ is asymptotically normal. For $N \in \mathbb{N}$ and $j \in \{0, \dots, N-1\}$ put

$$X_j := \begin{bmatrix} X_j^1 \\ X_j^2 \end{bmatrix} := \begin{bmatrix} \int_{2\pi j/\omega}^{2\pi(j+1)/\omega} \cos(\omega t) dL(t) \\ \int_{2\pi j/\omega}^{2\pi(j+1)/\omega} \sin(\omega t) dL(t) \end{bmatrix}.$$

Observe that X_j are independent and identically distributed random vectors with mean zero and the covariance matrix $\widetilde{\Sigma}_1 := \frac{\sigma^2 \pi}{\omega} I_{2 \times 2}$. Therefore,

$$\int_0^{\frac{2\pi N}{\omega}} e^{-i\omega t} dL(t) = \sum_{j=0}^{N-1} X_j.$$

Applying the classical CLT we obtain

$$\sqrt{N} \left(\frac{1}{N} \sum_{j=0}^{N-1} X_j \right) = \frac{1}{\sqrt{N}} \int_0^{\frac{2\pi N}{\omega}} e^{-i\omega t} dL(t) \rightarrow \mathcal{N} \sim \mathcal{N}(0, \widetilde{\Sigma}_1) \quad \text{as } N \rightarrow \infty.$$

So $\frac{\sqrt{\omega}}{\sqrt{2\pi N}} \int_0^{\frac{2\pi N}{\omega}} e^{-i\omega t} dL(t) \rightarrow \mathcal{N}(0, \Sigma_1)$, where $\Sigma_1 = \frac{\omega}{2\pi} \widetilde{\Sigma}_1 = \frac{\sigma^2}{2} I_{2 \times 2}$. Put

$$A := \begin{bmatrix} \Re \left(\frac{b(i\omega)}{a(i\omega)} \right) & \Im \left(\frac{b(i\omega)}{a(i\omega)} \right) \\ \Im \left(\frac{b(i\omega)}{a(i\omega)} \right) & -\Re \left(\frac{b(i\omega)}{a(i\omega)} \right) \end{bmatrix}.$$

Observe that

$$A \cdot \begin{bmatrix} \frac{\sqrt{\omega}}{\sqrt{2\pi N}} \int_0^{2\pi N/\omega} \cos(\omega t) dL(t) \\ \frac{\sqrt{\omega}}{\sqrt{2\pi N}} \int_0^{2\pi N/\omega} \sin(\omega t) dL(t) \end{bmatrix} = \begin{bmatrix} \Re Z(2\pi N) \\ \Im Z(2\pi N) \end{bmatrix}.$$

Thus $Z = A \cdot X$ is normally distributed with mean zero and the covariance matrix $\Sigma = A \Sigma_1 A^T = \frac{\sigma^2}{2} \left| \frac{b(i\omega)}{a(i\omega)} \right|^2 I_{2 \times 2}$. \square

Now we apply this theorem to find the asymptotic distribution of the truncated Fourier transform squared.

Theorem 3.7. *Let \mathbf{X} and Y be processes given by the state-space representation (2) and (3). Suppose that Assumptions 2.1 and 2.3 are satisfied. Let Z be defined as in Theorem 3.6. Then $|Z|^2 \sim \text{Exp}\left(\sigma^2 \left|\frac{b(i\omega)}{a(i\omega)}\right|^2\right)$, where $\text{Exp}(\lambda)$ denotes the exponential distribution with mean λ .*

PROOF We use the notation of the proof of Theorem 3.6. Thus $|Z|^2$ is proportional to chi-square random variables with two degrees of freedom, i.e. $|Z|^2 = \frac{\sigma^2}{2} \left|\frac{b(i\omega)}{a(i\omega)}\right|^2 X$, where $X \sim \chi^2(2)$. Thus $|Z|^2 \sim \Gamma\left(1, \frac{\sigma^2}{2} \left|\frac{b(i\omega)}{a(i\omega)}\right|^2\right)$ so $|Z|^2 \sim \text{Exp}\left(\sigma^2 \left|\frac{b(i\omega)}{a(i\omega)}\right|^2\right)$. \square

Now we are going to give the description of the convergence of the random vector consisting of the truncated Fourier transform at different frequencies.

Theorem 3.8. *Let \mathbf{X} and Y be processes given by the state-space representation (2) and (3). Suppose that Assumptions 2.1, 2.2 and 2.3 are satisfied. Let $0 < \omega_1 < \dots < \omega_d$ be fixed frequencies. Then $[\Re(\mathcal{F}_T(Y)(\omega_j)), \Im(\mathcal{F}_T(Y)(\omega_j))]_{j=1,\dots,d}^T$ converges to $\mathcal{N}\left(0, \frac{\sigma^2}{2} \mathbf{B}\right)$, with*

$$\mathbf{B} = \text{diag}\left(\left|\frac{b(i\omega_1)}{a(i\omega_1)}\right|^2, \left|\frac{b(i\omega_1)}{a(i\omega_1)}\right|^2, \dots, \left|\frac{b(i\omega_d)}{a(i\omega_d)}\right|^2, \left|\frac{b(i\omega_d)}{a(i\omega_d)}\right|^2\right)$$

and $[\mathcal{F}_T(\omega_j)]_{j=1,\dots,d}^T$ converges to a random vector whose coordinates are independent $\text{Exp}\left(\sigma^2 \left|\frac{b(i\omega_j)}{a(i\omega_j)}\right|^2\right)$ distributed random variables for $j = 1, \dots, d$.

PROOF For fixed $n \in \mathbb{N}$ and $k = 1, \dots, n$, put

$$X_k^{(2i-1)}(\omega_i) := \int_{2(k-1)\pi}^{2k\pi} \cos(\omega_i t) dL(t), \quad X_k^{(2i)}(\omega_i) := \int_{2(k-1)\pi}^{2k\pi} \sin(\omega_i t) dL(t), \quad i = 1, \dots, d.$$

Let $(s_n^{(2i-1)})^2 = \sum_{k=1}^n \text{Var}[X_k^{(2i-1)}(\omega_i)]$ and $(s_n^{(2i)})^2 = \sum_{k=1}^n \text{Var}[X_k^{(2i)}(\omega_i)]$. Put

$$Z_n^{(2i-1)}(\omega_i) := \frac{\sum_{k=1}^n X_k^{(2i-1)}(\omega_i)}{s_n^{(2i-1)}}, \quad Z_n^{(2i)}(\omega_i) := \frac{\sum_{k=1}^n X_k^{(2i)}(\omega_i)}{s_n^{(2i)}}.$$

Then we will show that by the Cramer-Wold-device the random vector $\mathbf{Z} \in \mathbb{R}^{2d}$ with $\mathbf{Z} = [Z_n^{(2i-1)}(\omega_i), Z_n^{(2i)}(\omega_i)]_{i=1,\dots,d}^T$ converges in distribution to $\mathcal{N}(0, I_{2d \times 2d})$.

We first apply the Lindeberg-Feller Central Limit Theorem (see e.g. Billingsley [2]) to each coordinate of the vector \mathbf{Z} . Observe that for all $i = 1, \dots, d$ by the Itô isometry we obtain

$$\begin{aligned} \text{Var}\left(X_k^{(2i-1)}(\omega_i)\right) &= \text{Var}\left(\int_{2(k-1)\pi}^{2k\pi} \cos(\omega_i t) dL(t)\right) = \sigma^2 \int_{2(k-1)\pi}^{2k\pi} \cos^2(\omega_i t) dt \\ &= \sigma^2 \frac{4\pi\omega_i + \sin(4\pi\omega_i k) - \sin(4\pi\omega_i(k-1))}{4\omega_i}. \end{aligned}$$

Thus

$$(s_n^{(2i-1)})^2 = \sum_{k=1}^n \text{Var}\left[X_k^{(2i-1)}(\omega_i)\right] = \sigma^2 \frac{4n\pi\omega_i + \sin(4\pi\omega_i n)}{4\omega_i}.$$

In the same way,

$$\left(s_n^{(2i)}\right)^2 = \sum_{k=1}^n \text{Var} \left[X_k^{(2i)}(\omega_i) \right] = \sigma^2 \frac{4n\pi\omega_i - \sin(4\pi\omega_i n)}{4\omega_i}.$$

Observe that

$$\lim_{n \rightarrow \infty} \frac{1}{n} \left(s_n^{(2i-1)}\right)^2 = \lim_{n \rightarrow \infty} \frac{1}{n} \left(s_n^{(2i)}\right)^2 = \sigma^2 \pi.$$

If the Lindeberg condition is satisfied, the $2i$ -th, respectively $2i - 1$ -th coordinate of \mathbf{Z} for $i = 1, \dots, d$, i.e.

$$\begin{aligned} Z_n^{(2i-1)}(\omega_i) &= \frac{2\sqrt{\omega_i}}{\sigma\sqrt{4\pi n\omega_i + \sin(4\pi n\omega_i)}} \int_0^{2\pi n} \cos(\omega_i t) dL(t) \\ Z_n^{(2i)}(\omega_i) &= \frac{2\sqrt{\omega_i}}{\sigma\sqrt{4\pi n\omega_i - \sin(4\pi n\omega_i)}} \int_0^{2\pi n} \sin(\omega_i t) dL(t) \end{aligned}$$

converges to $\mathcal{N}(0, 1)$. Taking

$$Y_n^{(2i-1)}(\omega_i) = \frac{\sigma\sqrt{4\pi n\omega_i + \sin(4\pi n\omega_i)}}{2\sqrt{2\pi n\omega_i}}, \quad Y_n^{(2i)}(\omega_i) = \frac{\sigma\sqrt{4\pi n\omega_i - \sin(4\pi n\omega_i)}}{2\sqrt{2\pi n\omega_i}}$$

and noting that

$$\lim_{n \rightarrow \infty} Y_n^{(2i-1)}(\omega_i) = \frac{\sigma}{\sqrt{2}}, \quad \lim_{n \rightarrow \infty} Y_n^{(2i)}(\omega_i) = \frac{\sigma}{\sqrt{2}}$$

is constant at all frequencies, by Slutsky arguments for $i = 1, \dots, d$ we get

$$(21) \quad \frac{1}{\sqrt{2\pi n}} \int_0^{2\pi n} \cos(\omega_i t) dL(t) = Z_n^{(2i-1)}(\omega_i) Y_n^{(2i-1)}(\omega_i) \rightarrow \mathcal{N}\left(0, \frac{\sigma^2}{2}\right),$$

$$(22) \quad \frac{1}{\sqrt{2\pi n}} \int_0^{2\pi n} \sin(\omega_i t) dL(t) = Z_n^{(2i)}(\omega_i) Y_n^{(2i)}(\omega_i) \rightarrow \mathcal{N}\left(0, \frac{\sigma^2}{2}\right).$$

Now we are going to prove the Lindeberg condition for odd coordinates of \mathbf{Z} (for the even ones an analogous reasoning holds), i.e. for all $\epsilon > 0$ it holds

$$\lim_{n \rightarrow \infty} \frac{1}{\left(s_n^{(2i-1)}\right)^2} \sum_{k=1}^n \mathbb{E} \left[\left(X_k^{(2i-1)}(\omega_i) \right)^2 \mathbf{1}_{\left\{ |X_k^{(2i-1)}(\omega_i)| > \epsilon s_n^{(2i-1)} \right\}} \right] = 0.$$

Observe that if the random variables $\{X_k^{(2i-1)}(\omega_i)\}$ are uniformly square integrable, then they satisfy the Lindeberg condition. Indeed,

$$\begin{aligned} & \left(s_n^{(2i-1)}\right)^{-2} \sum_{k=1}^n \mathbb{E} \left[\left(X_k^{(2i-1)}(\omega_i) \right)^2 \mathbf{1}_{\left\{ |X_k^{(2i-1)}(\omega_i)| > \epsilon s_n^{(2i-1)} \right\}} \right] \\ &= \left(s_n^{(2i-1)}\right)^{-2} \sum_{k=1}^n \mathbb{E} \left[\left(X_k^{(2i-1)}(\omega_i) \right)^2 \mathbf{1}_{\left\{ |X_k^{(2i-1)}(\omega_i)|^2 > \left(\epsilon s_n^{(2i-1)}\right)^2 \right\}} \right] \\ &\leq \left(s_n^{(2i-1)}\right)^{-2} n \sup_{k=1, \dots, n} \mathbb{E} \left[\left(X_k^{(2i-1)}(\omega_i) \right)^2 \mathbf{1}_{\left\{ |X_k^{(2i-1)}(\omega_i)|^2 > \left(\epsilon s_n^{(2i-1)}\right)^2 \right\}} \right] \\ &= \left(\sigma^2 \frac{4n\pi\omega_i + \sin(4\pi\omega_i n)}{4\omega_i} \right)^{-1} n \sup_{k=1, \dots, n} \mathbb{E} \left[\left(X_k^{(2i-1)}(\omega_i) \right)^2 \mathbf{1}_{\left\{ |X_k^{(2i-1)}(\omega_i)|^2 > \left(\epsilon s_n^{(2i-1)}\right)^2 \right\}} \right] \end{aligned}$$

Since $\lim_{n \rightarrow \infty} \left(\sigma^2 \frac{4n\pi\omega_i + \sin(4\pi\omega_i n)}{4\omega_i} \right)^{-1} n \rightarrow \frac{1}{\pi\sigma^2}$, uniform square integrability implies in this case the Lindeberg condition. It remains to show the uniform square integrability of $\left\{ X_k^{(2i-1)}(\omega_i) \right\}_{k \in \mathbb{N}}$.

Assume first, that our driving process $(L(t))_{t \geq 0}$ is of bounded variation. Then

$$M_k = \left| \int_{2(k-1)\pi}^{2k\pi} \cos(\omega_i t) dL_t \right| \leq \int_{2(k-1)\pi}^{2k\pi} |\cos(\omega_i t)| d|L_t| \leq \int_{2(k-1)\pi}^{2k\pi} d|L_t|,$$

where $|\cdot|$ denotes the total variation of the process. But $\int_{2(k-1)\pi}^{2k\pi} d|L_t| \stackrel{d}{=} \int_0^{2\pi} d|L_t|$. We have

$$\begin{aligned} \mathbb{E} \left[|M_k|^2 \mathbf{1}_{\{|M_k| > K\}} \right] &\leq \mathbb{E} \left[\left| \int_{2(k-1)\pi}^{2k\pi} d|L_t| \right|^2 \mathbf{1}_{\left\{ \left| \int_{2(k-1)\pi}^{2k\pi} d|L_t| \right| > K \right\}} \right] \\ &= \mathbb{E} \left[\left| \int_0^{2\pi} d|L_t| \right|^2 \mathbf{1}_{\left\{ \left| \int_0^{2\pi} d|L_t| \right| > K \right\}} \right]. \end{aligned}$$

By the square integrability of $\int_0^{2\pi} d|L_t|$, which is implied by the square integrability of $(L(t))_{t \geq 0}$ we obtain the uniform integrability of $(M_k)_{k \in \mathbb{N}}$.

Now we assume that $(L(t))$ is a square integrable martingale with finite moments of all orders. Observe that X_k is square integrable for all $k \in \mathbb{N}$. By the Burkholder-Davis-Gundy Inequality (see e.g. Protter [20]) for each $p \geq 1$ there exists a positive constant C_p such that

$$\mathbb{E} \left[\left(\int_{2(k-1)\pi}^{2k\pi} \cos(\omega_i t) dL(t) \right)^p \right] \leq C_p \mathbb{E} \left[\left[\int_{2(k-1)\pi}^{2k\pi} \cos(\omega_i t) dL(t), \int_{2(k-1)\pi}^{2k\pi} \cos(\omega_i t) dL(t) \right]^{p/2} \right].$$

Since

$$\left[\int_{2(k-1)\pi}^{2k\pi} \cos(\omega_i t) dL(t), \int_{2(k-1)\pi}^{2k\pi} \cos(\omega_i t) dL(t) \right] = \int_{2(k-1)\pi}^{2k\pi} \cos^2(\omega_i t) d[L, L]_t$$

using the above inequality for $p = 4$ we obtain

$$\begin{aligned} \mathbb{E} \left[\left(\int_{2(k-1)\pi}^{2k\pi} \cos(\omega_i t) dL(t) \right)^4 \right] &\leq C_4 \mathbb{E} \left[\int_{2(k-1)\pi}^{2k\pi} \cos^2(\omega_i t) d[L, L]_t \right] \\ &\leq \sigma^2 \int_{2(k-1)\pi}^{2k\pi} \cos^2(\omega_i t) dt < C \end{aligned}$$

for some constant C . Since $\{X_k^{(2i-1)}(\omega_i)\}$ are square integrable and $\{X_k^{(2i-1)}(\omega_i)\}$ are bounded in $L^4(\Omega, \mathcal{F}, \mathbb{P})$ they are uniformly square integrable.

As any Lévy process is by the Lévy-Itô decomposition the sum of a finite variation Lévy process and an independent square integrable martingale with moments of all orders, we obtain the claimed uniform square integrability for all driving Lévy processes.

Likewise one shows that $\theta^T Z$ converges in distribution to $\mathcal{N}\left(0, \frac{\sigma^2}{2} \theta^T \theta\right)$ for all $\theta \in \mathbb{R}^{2d}$. So the Cramer-Wold device concludes.

Therefore $\left[Z_n^{(2i-1)}(\omega_i) Y_n^{(2i-1)}(\omega_i), Z_n^{(2i)}(\omega_i) Y_n^{(2i)}(\omega_i) \right]_{i=1, \dots, d}^T$ converges in distribution to $\mathcal{N}\left(0, \frac{\sigma^2}{2} I_{2d \times 2d}\right)$ and thus using Lemma 3.4 and equations (21), (22) $[\mathcal{F}_T(\omega_j)]_{j=1, \dots, d}^T$ converges to $\mathcal{N}\left(0, \frac{\sigma^2}{2} \mathbf{B}\right)$, where \mathbf{B} is defined above. Repeating the reasoning from the proof of Theorem 3.7 we obtain that $[|\mathcal{F}_T(\omega_j)|^2]_{j=1, \dots, d}^T$ converges to a vector of independent, exponentially distributed random variables with $\text{Exp}\left(\sigma^2 \left| \frac{b(i\omega_j)}{a(i\omega_j)} \right|^2\right)$ for $j = 1, \dots, d$. \square

Note that Theorem 3.6 is basically a special case of Theorem 3.8. However, the proof in the case of several frequencies is much more complicated and a more elementary reasoning was also presented.

The limiting result is the analogue of the one for discrete time ARMA models. (See e.g. [7] Chapter 10.)

3.2. Numerical Approximation of Integrals and Limiting Behaviour of the Truncated Pathwise Fourier Transform Based on Non-equidistant Discrete Grids.
In this section we deal with the numerical approximation of the integral

$$(23) \quad \mathcal{F}_T(Y)(\omega) := \frac{1}{\sqrt{T}} \int_0^T Y(t) e^{-i\omega t} dt.$$

Our aim is to describe conditions under which we are able to calculate numerically the truncated Fourier transform of a CARMA process based on non-equidistant observations. The main result is the following:

Theorem 3.9. *Let \mathbf{X} and Y be processes given by the state-space representation (2) and (3). Suppose that Assumptions 2.1, 2.2, 2.3 and 2.4 are satisfied. Assume that $F: \mathbb{R} \rightarrow \mathbb{R}^d$ be a twice continuously differentiable function with $\|F''\|_\infty < \infty$. Let $(x_i^{(T)})_{i=0, \dots, N(T)-2}$ be a partition of the interval $[a, b]$ with $x_0^{(T)} = a$ and $x_{N(T)-1}^{(T)} = b$ and let $h_{\max}(T) = \max_{j=0, \dots, N(T)-1} (x_{j+1}^{(T)} - x_j^{(T)})$. Put*

$$(24) \quad \alpha_0^{(N(T))} = \frac{x_1^{(T)} - x_0^{(T)}}{2} F(x_0^{(T)}), \quad \alpha_{N(T)-1}^{(N(T))} = \frac{x_{N(T)-1}^{(T)} - x_{N(T)-2}^{(T)}}{2} F(x_{N(T)-1}^{(T)}),$$

$$(25) \quad \alpha_j^{(N(T))} = \frac{x_{j+1}^{(T)} - x_{j-1}^{(T)}}{2} F(x_j^{(T)}), \quad j = 1, \dots, N(T) - 2.$$

Then there exist positive constants C_1, C_2 such that

$$\mathbb{E} \left[\left\| \sum_{j=0}^{N(T)-1} \alpha_j^{(N(T))} Y(x_j^{(T)}) - \int_a^b Y(t) F(t) dt \right\|^2 \right] \leq C_1 (C_2 + T) N(T)^2 h_{\max}^6(T)$$

and thus if $\lim_{T \rightarrow \infty} T N(T)^2 h_{\max}^6(T) = 0$, then

$$\lim_{T \rightarrow \infty} \left\| \sum_{j=0}^{N(T)-1} \alpha_j^{(N(T))} F(x_j^{(T)}) - \int_a^b Y(t) F(t) dt \right\|_{L^2} = 0.$$

We begin by establishing an error bound of the trapezoidal method for non-equidistant data. For a very accessible approach of quadrature rules procedures we refer to [22]. Recall the basic properties of the trapezoidal rule:

Lemma 3.10. *Let $f: [a, b] \rightarrow \mathbb{R}$ be a twice continuously differentiable function. Write*

$$(26) \quad \int_a^b f(x)dx = \frac{b-a}{2}[f(a) + f(b)] + E^T(f).$$

Then

$$(27) \quad |E^T(f)| \leq \frac{(b-a)^3}{12} \sup_{x \in [a,b]} |f''(x)|.$$

For the composite trapezoidal rule for an equidistant grid $a < a + (b-a)\frac{1}{n} < \dots, a + (b-a)\frac{i}{n} < \dots < b$ we have

$$(28) \quad \int_a^b f(x)dx = \frac{b-a}{2n} \left[f(a) + 2 \sum_{i=1}^{n-1} f\left(a + (b-a)\frac{i}{n}\right) + f(b) \right] + E_n^T(f).$$

Then

$$(29) \quad |E_n^T(f)| \leq \frac{(b-a)^3}{12n^2} \sup_{x \in [a,b]} |f''(x)|.$$

A proof can be found e.g. in [22].

Now we are going to formulate a version of the trapezoidal rule for non-equidistant points. We assume that we have some control on the maximal distance between observations.

Lemma 3.11. *Let $a = x_0 < x_1 < \dots < x_{N-1} < x_N = b$ be an arbitrary partition of the interval $[a, b]$ and assume that $f: [a, b] \rightarrow \mathbb{R}$ is a twice continuously differentiable function. Put $h_{\max} = \max_{j=0, \dots, N-2} (x_{j+1} - x_j)$. Then*

$$\int_a^b f(x)dx = \sum_{j=0}^{N-1} \frac{x_{j+1} - x_j}{2} [f(x_j) + f(x_{j+1})] + E^T(f),$$

where $|E^T(f)| \leq N \|f''\|_{\infty} \frac{h_{\max}^3}{12}$.

PROOF

Let us write

$$[a, b] = \bigcup_{j=0}^{N-1} [x_j, x_{j+1}], \quad I_j := [x_j, x_{j+1}]$$

and apply Lemma 3.10 for each interval I_j . Therefore

$$\int_{x_j}^{x_{j+1}} f(x)dx = \frac{x_{j+1} - x_j}{2} [f(x_j) + f(x_{j+1})] + E_j^T(f),$$

with

$$|E_j^T(f)| \leq \frac{|x_{j+1} - x_j|^3}{12} \sup_{x \in [x_j, x_{j+1}]} |f''(x)|.$$

For each $i = 0, 1, \dots, N-1$ we have

$$\sup_{x \in [x_j, x_{j+1}]} |f''(x)| \leq \sup_{x \in [a, b]} |f''(x)| =: \|f''\|_{\infty}.$$

Therefore

$$\int_a^b f(x)dx = \sum_{i=0}^{N-1} \frac{x_{j+1} - x_j}{2} [f(x_j) + f(x_{j+1})] + E^T(f),$$

where

$$\begin{aligned} |E^T(f)| &= \left| \sum_{i=0}^{N-1} E_j^T(f) \right| \leq \|f''\|_\infty \sum_{i=0}^{N-1} \frac{(x_{j+1} - x_j)^3}{12} \\ &\leq \|f''\|_\infty \sum_{i=0}^{N-1} \frac{h_{\max}^3}{12} = N \|f''\|_\infty \frac{h_{\max}^3}{12}. \end{aligned}$$

This completes the proof. \square

We use some results and ideas from [10]. The aim is to find an approximation similar to Proposition 5.4 of [10] of the integral appearing in the truncated Fourier transform in the case that the observations of the process Y are given on a non-equidistant grid. Let

$$T_{[0,T]}^N f = \sum_{j=0}^{N-1} \frac{x_{j+1} - x_j}{2} [f(x_j) + f(x_{j+1})]$$

be the trapezoidal rule discussed in Lemma 3.11. Recall first the Fubini type theorem for stochastic integrals from [10].

Lemma 3.12. [10, Theorem 2.4] *Let $[a, b] \subset \mathbb{R}$ be a bounded interval and $(L(t))_{t \geq 0}$ be a Lévy process with finite second moments. Assume that $F: [a, b] \times \mathbb{R} \rightarrow \mathbb{R}^d$ is a bounded function $\mathcal{B}([a, b]) \otimes \mathcal{B}([-s, t])$ -measurable for all $s, t \in (0, \infty)$ and the family $\{u \mapsto F(s, u)\}_{u \in [a, b]}$ is uniformly absolutely integrable and uniformly converges to zero as $|u| \rightarrow 0$. Then*

$$(30) \quad \int_a^b \int_{\mathbb{R}} F(s, u) dL(u) ds = \int_{\mathbb{R}} \int_a^b F(s, u) ds dL(u) \quad a.s.$$

In the paper [10] the assumption about measurability in the statement of the theorem is not explicitly stated. However, an inspection of their proof combined with results from [23] shows that the precise statement has to be in the above form.

Secondly, note that for non-equidistant data the corresponding error estimation [10, Proposition A.6] has the following form:

Proposition 3.13. *Let $[a, b] \subset \mathbb{R}$ be a compact interval and use the notation of Lemma 3.11.*

(1) *If $f: [a, b] \rightarrow \mathbb{R}$ is twice continuously differentiable, then*

$$\left| \int_a^b f(s) ds - T_{[a,b]}^N f \right| \leq N \|f''\|_\infty \frac{h_{\max}^3}{12}.$$

(2) *If $F: [a, b] \rightarrow \mathbb{R}^d$ is twice continuously differentiable, then*

$$\left\| \int_a^b F(s) ds - T_{[a,b]}^N F \right\| \leq \sqrt{d} N \|F''\|_\infty \frac{h_{\max}^3}{12},$$

where $\|\cdot\|$ denotes the Euclidean norm in \mathbb{R}^d .

Here $\|F''\|_\infty := \max_{i=1, \dots, d} \sup_{t_i \in [a, b]} \|F''(t_i)\|$.

Put

$$E_{fg}^{T,N} := T_{[0,T]}^N f(\cdot)g(\cdot) - \int_0^T g(s)f(s)ds.$$

PROOF OF THEOREM 3.9. Assume that we have observed the process Y on the grid $0 = x_0^{(T)} < x_1^{(T)} < \dots < x_{N(T)-1}^{(T)} = T$. We have

$$(31) \quad T_{[0,T]}^N FY = \sum_{j=0}^{N(T)-1} \alpha_j^{(N(T))} Y(x_j^{(T)}),$$

where $\alpha_j^{(N(T))}$ ($j = 0, \dots, N(T) - 1$) are the coefficients given by (24) and (25).

Observe that $f(a) = \int f(s)\delta_a(s)ds$. Moreover, for all $j = 0, \dots, N(T) - 1$ we know that $x_j^{(T)} \in [0, T]$, therefore for all $u \in [0, T]$ and for all $j = 0, \dots, N(T) - 1$ we have

$$\mathbf{1}_{[u,T]}(x_j^{(T)}) = \mathbf{1}_{[0,x_j^{(T)}]}(u).$$

Thus by (31) we have

$$\begin{aligned} T_{[0,T]}^N FY &= \sum_{j=0}^{N(T)-1} \alpha_j^{(N(T))} Y(x_j^{(T)}) = \sum_{j=0}^{N(T)-1} \alpha_j^{(N(T))} \int_{-\infty}^{x_j^{(T)}} \mathbf{b}^T e^{\mathbf{A}(x_j^{(T)}-u)} \mathbf{e} dL^*(u) \\ &= \sum_{j=0}^{N(T)-1} \alpha_j^{(N(T))} \left(\int_{-\infty}^0 \mathbf{b}^T e^{\mathbf{A}(x_j^{(T)}-u)} \mathbf{e} dL^*(u) + \int_0^{x_j^{(T)}} \mathbf{b}^T e^{\mathbf{A}(x_j^{(T)}-u)} \mathbf{e} dL^*(u) \right) \\ &= \int_{-\infty}^0 \sum_{j=0}^{N(T)-1} \alpha_j^{(N(T))} \mathbf{b}^T e^{\mathbf{A}(x_j^{(T)}-u)} \mathbf{e} dL^*(u) \\ &\quad + \int_0^T \sum_{j=0}^{N(T)-1} \alpha_j^{(N(T))} \mathbf{b}^T e^{\mathbf{A}(x_j^{(T)}-u)} \mathbf{e} \mathbf{1}_{[0,x_j^{(T)}]}(u) dL^*(u) \\ &= \int_{-\infty}^0 \sum_{j=0}^{N(T)-1} \alpha_j^{(N(T))} \mathbf{b}^T e^{\mathbf{A}(x_j^{(T)}-u)} \mathbf{e} dL^*(u) \\ &\quad + \int_0^T \sum_{j=0}^{N(T)-1} \alpha_j^{(N(T))} \mathbf{b}^T e^{\mathbf{A}(x_j^{(T)}-u)} \mathbf{e} \mathbf{1}_{[u,T]}(x_j^{(T)}) dL^*(u) \\ &= \int_{-\infty}^0 \int_0^T \sum_{j=0}^{N(T)-1} \alpha_j^{(N(T))} \delta_{x_j^{(T)}}(s) \mathbf{b}^T e^{\mathbf{A}(s-u)} \mathbf{e} ds dL^*(u) \\ &\quad + \int_0^T \int_u^T \sum_{j=0}^{N(T)-1} \alpha_j^{(N(T))} \delta_{x_j^{(T)}}(s) \mathbf{b}^T e^{\mathbf{A}(s-u)} \mathbf{e} ds dL^*(u) \\ &= \int_{-\infty}^T \int_{\max\{0,u\}}^T \sum_{j=0}^{N(T)-1} \alpha_j^{(N(T))} \delta_{x_j^{(T)}}(s) \mathbf{b}^T e^{\mathbf{A}(s-u)} \mathbf{e} ds dL^*(u). \end{aligned}$$

Thus using the representation (6) and the Fubini-type Theorem 3.12 we have

$$\int_0^T F(s)Y(s)ds = \int_0^T F(s) \int_{-\infty}^s \mathbf{b}^T e^{\mathbf{A}(s-u)} \mathbf{e} dL^*(u) ds$$

$$\begin{aligned}
&= \int_{-\infty}^T \int_{\max\{0,u\}}^T F(s) \mathbf{b}^T e^{\mathbf{A}(s-u)} \mathbf{e} ds dL^*(u) \\
&= \int_{-\infty}^0 \int_0^T F(s) \mathbf{b}^T e^{\mathbf{A}(s-u)} \mathbf{e} ds dL^*(u) \\
&+ \int_0^T \int_u^T F(s) \mathbf{b}^T e^{\mathbf{A}(s-u)} \mathbf{e} ds dL^*(u).
\end{aligned}$$

Thus

$$\begin{aligned}
E_{FY}^{T,N} &= T_{[0,T]}^N FY - \int_0^T F(s) Y(s) ds = \int_0^T \left(\sum_{j=0}^{N(T)-1} \alpha_j^{(N(T))} \delta_{x_j^{(T)}}(s) - F(s) \right) Y(s) ds \\
&= \int_{-\infty}^0 \int_0^T \left(\sum_{j=0}^{N(T)-1} \alpha_j^{(N(T))} \delta_{x_j^{(T)}}(s) - F(s) \right) \mathbf{b}^T e^{\mathbf{A}(s-u)} \mathbf{e} ds dL^*(u) \\
&+ \int_0^T \int_u^T \left(\sum_{j=0}^{N(T)-1} \alpha_j^{(N(T))} \delta_{x_j^{(T)}}(s) - F(s) \right) \mathbf{b}^T e^{\mathbf{A}(s-u)} \mathbf{e} ds dL^*(u).
\end{aligned}$$

Let us denote

$$(32) \quad \Gamma^{(N)}(u) := \int_0^T \left(\sum_{j=0}^{N(T)-1} \alpha_j^{(N(T))} \delta_{x_j^{(T)}}(s) - F(s) \right) \mathbf{b}^T e^{\mathbf{A}(s-u)} \mathbf{e} ds, \quad u \leq 0,$$

$$(33) \quad G^{(N)}(u) := \int_u^T \left(\sum_{j=0}^{N(T)-1} \alpha_j^{(N(T))} \delta_{x_j^{(T)}}(s) - F(s) \right) \mathbf{b}^T e^{\mathbf{A}(s-u)} \mathbf{e} ds, \quad u \in [0, T].$$

By Assumption 2.3 we know that there exist positive constants α, β such that

$$(34) \quad \|\exp(\mathbf{A}t)\| \leq \beta \exp(-\alpha t).$$

Note that by Lemma 3.11 and Proposition 3.13 we have

$$\begin{aligned}
&\left\| \int_{u_0}^T \left(\sum_{j=0}^{N(T)-1} \alpha_j^{(N(T))} \delta_{x_j^{(T)}}(s) - F(s) \right) \mathbf{b}^T e^{\mathbf{A}(s-u)} \mathbf{e} ds \right\|_{\mathbb{R}^d} \\
&= \left\| \sum_{j=0}^{N(T)-1} \alpha_j^{(N(T))} \delta_{x_j^{(T)}}(s) \mathbf{b}^T e^{\mathbf{A}(x_j-u)} \mathbf{e} - \int_{u_0}^T F(s) \mathbf{b}^T e^{\mathbf{A}(s-u)} \mathbf{e} ds \right\|_{\mathbb{R}^d} \\
&\leq \sqrt{d} N(T) \|\tilde{F}''(u)\|_{\infty} \frac{h_{\max}^3(T)}{12}
\end{aligned}$$

with $\tilde{F}(s) = F(s) \mathbf{b}^T e^{\mathbf{A}(s-u)} \mathbf{e}$ and $u_0 \in [0, T]$. If $u_0 = 0$, then there exist $\tilde{\alpha} > 0$ and $D > 0$ such that $\|\tilde{F}''(u)\|_{\infty} \leq D \exp(\tilde{\alpha} u)$ for $u \leq 0$. Therefore there exists a constant $D_1 > 0$ such that

$$\|\Gamma^{(N)}(u)\|_{\mathbb{R}^d} \leq \sqrt{d} N(T) \|\tilde{F}\|_{[0,T]}''_{\infty} \frac{h_{\max}^3(T)}{12} \leq D_1 N(T) h_{\max}^3(T) \exp(\tilde{\alpha} u), \quad u \leq 0.$$

If now $u_0 = u$ is any element of $[0, T]$, then there exists $D > 0$ such that $\|\tilde{F}''\|_{[u,T]}_{\infty} \leq D$ for $u \in [0, T]$. Therefore there exists a constant $D_2 > 0$ such that for $u \in [0, T]$ we have

$$\|G^{(N)}(u)\|_{\mathbb{R}^d} \leq \sqrt{d} N(T) \|\tilde{F}\|_{[u,T]}''_{\infty} \frac{h_{\max}^3(T)}{12} \leq D_2 N(T) h_{\max}^3(T).$$

By the Itô isometry

$$\begin{aligned}
\left\| \int_{-\infty}^0 \Gamma^{(N)}(u) dL^*(u) \right\|_{L^2}^2 &= \mathbb{E} \left[\left(\int_{-\infty}^0 \Gamma^{(N)}(u) dL^*(u) \right)^T \left(\int_{-\infty}^0 \Gamma^{(N)}(u) dL^*(u) \right) \right] \\
&= \mathbb{E} \left[\left(\int_{-\infty}^0 \Gamma^{(N)}(u) dL^*(u) \right)^T \left(\int_{-\infty}^0 \Gamma^{(N)}(u) dL^*(u) \right) \right] \\
&= \sigma^2 \left(\int_{-\infty}^0 [\Gamma^{(N)}(u)]^T \Gamma^{(N)}(u) du \right) \\
&\leq \sigma^2 \int_{-\infty}^0 \|\Gamma^{(N)}(u)\|_{\mathbb{R}^d}^2 du \\
&\leq \sigma^2 \int_{-\infty}^0 (D_1 N(T) h_{\max}^3(T) \exp(\tilde{\alpha} u))^2 du \\
&= \sigma^2 N(T)^2 h_{\max}^6(T) D_1^2 \int_{-\infty}^0 \exp(2\tilde{\alpha} u) du \\
&= D_\Gamma N(T)^2 h_{\max}^6(T),
\end{aligned}$$

where $D_\Gamma > 0$ is a constant. In a similar way we obtain

$$\begin{aligned}
\left\| \int_0^T G^{(N)}(u) dL(u) \right\|_{L^2}^2 &= \mathbb{E} \left[\left(\int_0^T G^{(N)}(u) dL(u) \right)^T \left(\int_0^T G^{(N)}(u) dL(u) \right) \right] \\
&= \mathbb{E} \left[\left(\int_0^T G^{(N)}(u) dL(u) \right)^T \left(\int_0^T G^{(N)}(u) dL(u) \right) \right] \\
&= \sigma^2 \left(\int_0^T [G^{(N)}(u)]^T G^{(N)}(u) du \right) \\
&\leq \sigma^2 \int_0^T \|G^{(N)}(u)\|_{\mathbb{R}^d}^2 du \leq \sigma^2 \int_0^T (D_2 N(T) h_{\max}^3(T))^2 du \\
&= D_G N(T)^2 T h_{\max}^6(T)
\end{aligned}$$

for some constant $D_G > 0$. Therefore

$$\|E_{FY}^{T,N}\|_{L^2}^2 \leq 2 \left[\left\| \int_{-\infty}^0 \Gamma^{(N)}(u) dL^*(u) \right\|_{L^2}^2 + \left\| \int_0^T G^{(N)}(u) dL(u) \right\|_{L^2}^2 \right],$$

thus

$$\|E_{FY}^{T,N}\|_{L^2}^2 \leq C_1 ((C_2 + T) N(T)^2 h_{\max}^6(T))^2,$$

where C_1, C_2 are positive constants. If $\lim_{T \rightarrow \infty} T N(T)^2 h_{\max}^6(T) = 0$, then $\lim_{T \rightarrow \infty} \|E_{FY}^{T,N}\|_{L^2}^2 = 0$. This completes the proof. \square

Now we are going to apply Theorem 3.9 to find a numerical approximation of the truncated Fourier transform. Using the notation of Theorem 3.9 we denote the trapezoidal approximation of

$$\mathcal{F}_T(Y)(\omega) = \frac{1}{\sqrt{T}} \int_0^T Y(t) e^{-i\omega t} dt$$

by $\mathcal{T}_T(Y)(\omega)$, i.e.

$$\mathcal{T}_T(Y)(\omega) = \frac{1}{\sqrt{T}} \sum_{j=0}^{N-1} \alpha_j^{(N)} Y(x_j^{(N)}),$$

where the grid points $(x_j^{(N)})_{j=0,\dots,N(T)-1}$ are given as in Theorem 3.9 and

$$\alpha_0^{(N(T))} = \frac{x_1^{(T)} - x_0^{(T)}}{2} F(x_0^{(T)}), \quad \alpha_{N(T)-1}^{(N(T))} = \frac{x_{N(T)-1}^{(T)} - x_{N(T)-2}^{(T)}}{2} F(x_{N(T)-1}^{(T)}),$$

$$\alpha_j^{(N(T))} = \frac{x_{j+1}^{(T)} - x_{j-1}^{(T)}}{2} F(x_j^{(T)}), \quad j = 1, \dots, N(T) - 2.$$

with $F(x) = e^{-i\omega x}$.

Theorem 3.14. *Let \mathbf{X} and Y be processes given by the state-space representation (2) and (3). Suppose that Assumptions 2.1, 2.2, 2.3 and 2.4 are satisfied and that the process Y is observed at not necessarily equidistant points $0 = x_0^{(T)} < x_1^{(T)} < \dots < x_{N(T)-1}^{(T)} = T$. Let $h_{\max}(T) := \max_{j=0,\dots,N(T)-2} (x_{j+1}^{(T)} - x_j^{(T)})$. If*

$$\lim_{T \rightarrow \infty} N(T) h_{\max}^3(T) = 0,$$

then

$$\lim_{T \rightarrow \infty} \|\mathcal{T}_T(Y)(\omega) - \mathcal{F}_T(Y)(\omega)\|_{L^2} = 0$$

and thus also

$$\mathbb{P} - \lim_{T \rightarrow \infty} [\mathcal{T}_T(Y)(\omega) - \mathcal{F}_T(Y)(\omega)] = 0.$$

PROOF We identify \mathbb{C} with \mathbb{R}^2 in the canonical way. Applying Theorem 3.9 for $d = 2$, $F(t) = [\cos(\omega t), -\sin(\omega t)]^T$ we get

$$\mathbb{E} \left[\left\| \sum_{j=0}^{N(T)-1} \alpha_j^{(N(T))} Y(x_j^{(T)}) - \int_0^T Y(t) \begin{bmatrix} \cos(\omega t) \\ -\sin(\omega t) \end{bmatrix} dt \right\|^2 \right] \leq C_1(C_2 + T)N(T)^2 h_{\max}^6(T).$$

Dividing both sides by $T > 0$ we obtain

$$\mathbb{E} \left[\left\| \sum_{j=0}^{N(T)-1} \frac{\alpha_j^{(N(T))}}{\sqrt{T}} Y(x_j^{(T)}) - \frac{1}{\sqrt{T}} \int_0^T Y(t) \begin{bmatrix} \cos(\omega t) \\ -\sin(\omega t) \end{bmatrix} dt \right\|^2 \right] \leq \frac{C_1 C_2}{T} + C_1 N(T)^2 h_{\max}^6(T).$$

Passing to the limit with $T \rightarrow \infty$ and using the assumption $\lim_{T \rightarrow \infty} N(T) h_{\max}^3(T) = 0$ we get the assertion. \square

Now we are going to state the central limit theorem for the truncated Fourier transform:

Theorem 3.15. *Let \mathbf{X} and Y be processes given by the state-space representation (2) and (3). Suppose that Assumptions 2.1, 2.2, 2.3 and 2.4 are satisfied and the process Y is observed at not necessarily equidistant points $0 = x_0^{(T)} < x_1^{(T)} < \dots < x_{N(T)-1}^{(T)} = T$. Let $h_{\max}(T) := \max_{j=0,\dots,N(T)-2} (x_{j+1}^{(T)} - x_j^{(T)})$. Let $\alpha_j^{(N)}$ be defined as in Theorem 3.9. Assume that*

$$\lim_{T \rightarrow \infty} N(T) h_{\max}^3(T) = 0.$$

Put $\Sigma = \frac{\sigma^2}{2} \left| \frac{b(i\omega)}{a(i\omega)} \right|^2 I_{2 \times 2}$. If $\omega \neq 0$, then

$$d - \lim_{T \rightarrow \infty} \begin{bmatrix} \Re(\mathcal{T}_T Y(\omega)) \\ \Im(\mathcal{T}_T Y(\omega)) \end{bmatrix} = \mathcal{N}(0, \Sigma),$$

$$d - \lim_{T \rightarrow \infty} (\Re(\mathcal{T}_T Y(\omega))^2 + \Im(\mathcal{T}_T Y(\omega))^2) = \text{Exp} \left(\sigma^2 \left| \frac{b(i\omega)}{a(i\omega)} \right|^2 \right).$$

If $\omega = 0$, then

$$d - \lim_{T \rightarrow \infty} \mathcal{T}_T Y(0) = \mathcal{N} \left(0, \left(\frac{b(0)}{a(0)} \right)^2 \sigma^2 \right)$$

and

$$d - \lim_{T \rightarrow \infty} \frac{1}{\sigma^2} \left| \frac{a(0)\mathcal{T}_T Y(0)}{b(0)} \right|^2 \sim \chi^2(1).$$

Clearly, an analogous statement using Theorem 3.8 holds for the joint distribution when the truncated Fourier transform is taken at different frequencies.

PROOF OF THEOREM 3.15. Put

$$Z(T) := \frac{1}{\sqrt{T}} \frac{b(i\omega)}{a(i\omega)} \int_0^T e^{-i\omega t} dL(t)$$

and consider the following two-dimensional random vectors:

$$\mathbf{Z}_n := \begin{bmatrix} \Re(Z(T)) \\ \Im(Z(T)) \end{bmatrix}, \quad \mathbf{U}_n := \begin{bmatrix} \Re(\mathcal{F}_T Y(\omega)) \\ \Im(\mathcal{F}_T Y(\omega)) \end{bmatrix}, \quad \mathbf{V}_n := \begin{bmatrix} \Re(\mathcal{T}_T Y(\omega)) \\ \Im(\mathcal{T}_T Y(\omega)) \end{bmatrix}.$$

Observe that it is enough to consider the above limits for $T = n$. By Lemma 3.4 we know that

$$\mathbb{P} - \lim_{n \rightarrow \infty} \|\mathbf{U}_n - \mathbf{Z}_n\| = \mathbf{0}.$$

From Theorem 3.6 we get

$$d - \lim_{n \rightarrow \infty} \mathbf{Z}_n = \mathcal{N}(0, \Sigma).$$

Therefore

$$d - \lim_{n \rightarrow \infty} \mathbf{U}_n = \mathcal{N}(0, \Sigma).$$

By Theorem 3.14 we have

$$\mathbb{P} - \lim_{n \rightarrow \infty} (\mathbf{V}_n - \mathbf{U}_n) = \mathbf{0}.$$

Therefore,

$$d - \lim_{n \rightarrow \infty} \mathbf{V}_n = \mathcal{N}(0, \Sigma).$$

In the same way we obtain

$$d - \lim_{n \rightarrow \infty} |\mathbf{Z}|^2 = \text{Exp} \left(\sigma^2 \left| \frac{b(i\omega)}{a(i\omega)} \right|^2 \right).$$

In order to obtain the assertion for $\omega = 0$ we repeat the above reasonings applying Theorem 3.5 instead of Theorem 3.4. \square

4. ILLUSTRATIVE SIMULATIONS

We now turn to a numerical illustration of the theoretical convergence results given in Section 3.2. We are looking at simulations of CARMA processes and their numerically approximated truncated Fourier transform over different time horizons and maximal grid widths. To illustrate the convergence to the asymptotic normal distribution we shall look at several frequencies and different driving Lévy processes, standard Brownian motion, a Variance Gamma process and a “two sided Poisson process”. Of course, the truncated Fourier transform of (Y_t) is obtained using the trapezoidal rule based on non-equidistant observations of the CARMA process (Y_t) given on the interval $[0, T]$. On an interval $[0, T]$ we

generate a non-equidistant grid in the following way: we fix the maximal distance $h_{\max}(T)$ between elements of the grid and from each interval $[i \cdot \frac{1}{2}h_{\max}(T), (i+1) \cdot \frac{1}{2}h_{\max}(T))$ for $i = 0, 1, \dots, N-1$ we draw a number according to the uniform distribution. This results in a non-equidistant grid with the number of points being $N(T) = 2T/h_{\max} + 1$.

For our simulations we used the R Project for Statistical Computing. For the simulation we first generate the non-equidistant grid by the above procedure and then join it with a regular grid of mesh 0.001, which is still on average five times finer than the non-equidistant grid of the largest time horizon considered. On this joint grid the CARMA process Y is simulated with a standard Euler scheme for the state space representation. Afterwards only the simulated values at the times of the original non-equidistant grid are used to compute the approximation of the truncated Fourier transform with the trapezoidal rule. In all cases we simulate 2000 independent paths of the CARMA process and compute the associated values of the truncated Fourier transform at the following frequencies:

$$[\omega_1, \omega_2, \omega_3, \omega_4] = [0, 0.1, 1, 10].$$

For the non-zero frequencies real and imaginary part have to be considered separately. However, in the following we look only at the real parts as the behaviour of the imaginary parts is most similar. Mainly, the results are presented via QQ-plots where the theoretical values follow the (limiting) law described in Theorem 3.15.

We are going to consider CARMA processes with the following autoregressive and moving average orders: $(p, q) = (1, 0)$, i.e. an Ornstein-Uhlenbeck type process, and $(p, q) = (2, 1)$. For the time horizon T and the maximum distance of the non-equidistant observation times we consider the pairs $(T = 10, h_{\max} = 0.1)$, $(T = 50, h_{\max} = 0.05)$ and $(T = 100, h_{\max} = 0.01)$.

For each case we consider three different driving Lévy noises: standard Brownian Motion, a Variance Gamma process and a “two sided Poisson process”. For the definition and properties of the Variance Gamma process we refer to [18] and references therein. We construct the process in the following way: $V_t = G_t^1 - G_t^2$, where G_t^1 and G_t^2 are independent Gamma processes with shape parameter 1 and scale parameter 4. Likewise the “two sided Poisson process” is the difference of two independent Poisson processes with rate 10, i.e. a compound Poisson process with rate 20 and jumps +1 and -1 both with probability 1/2.

Example 4.1. We consider the CAR(1) model. Then $\mathbf{A} = -a_1$ and

$$a(z) := z + a_1, \quad b(z) = b_0.$$

So the spectral density is

$$f(\omega) = \frac{\sigma^2}{2\pi} \left| \frac{b(i\omega)}{a(i\omega)} \right|^2 = \frac{\sigma^2}{2\pi} \frac{b_0^2}{\omega^2 + a_1^2}.$$

For the simulations we take $[b_0, a_1] = [1, 2]$.

QQ-plots showing the results for 2000 simulated paths for the four different frequencies and three different combinations of time horizon and maximum grid width can be found in Figures 1, 2 and 3 for the driving Lévy process being a standard Brownian motion, a Variance Gamma and a two-sided Poisson process, respectively.

Example 4.2. We consider the CARMA(2, 1) model. We have

$$\mathbf{A} := \begin{bmatrix} 0 & 1 \\ -a_2 & -a_1 \end{bmatrix}, \quad \mathbf{b} := \begin{bmatrix} b_0 \\ 1 \end{bmatrix}, \quad \mathbf{e} := \begin{bmatrix} 0 \\ 1 \end{bmatrix}, \quad \mathbf{X}_t := \begin{bmatrix} X(t) \\ X^{(1)}(t) \end{bmatrix}$$

The autoregressive and moving-average polynomials are of the form

$$a(z) = z^2 + a_1z + a_2, \quad b(z) = z + b_0.$$

We have

$$\frac{b(i\omega)}{a(i\omega)} = \frac{i\omega + b_0}{(i\omega)^2 + (i\omega)a_1 + a_2}, \quad f(\omega) = \frac{\sigma^2}{2\pi} \left| \frac{b(i\omega)}{a(i\omega)} \right|^2 = \frac{\sigma^2}{2\pi} \frac{b_0^2 + \omega^2}{\omega^4 + (a_1^2 - 2a_2)\omega^2 + a_2^2}$$

For the simulation procedure we take $[b_0, b_1, a_1, a_2] = [1, 1, 1, 2]$.

QQ-plots showing the results for 2000 simulated paths for the four different frequencies and three different combinations of time horizon and maximum grid width can be found in Figures 4, 6 and 8 for the driving Lévy process being a standard Brownian motion, a Variance Gamma and a two-sided Poisson process, respectively. Likewise, Figures 5, 7 and 9 show corresponding histograms.

The simulation results seem to indicate the following.

In Figure 1 we notice at first a pretty good fit of the empirical quantiles from the simulations with the theoretical ones of the asymptotic distribution across all time horizons and frequencies. Looking more carefully, the fit in the tails clearly improves when the time horizon/fineness of the grid increases, but it is never bad. For the longest time horizon and finest grid the fit is clearly very good. Of course, it should not be forgotten that in this case the distribution of the (trapezoidal approximation of the) truncated Fourier transform is always exactly Gaussian and not only asymptotically. When looking across the non-zero frequencies one notes that for the shortest time horizon the quantiles for the smallest frequency 0.1 appear to lie on a line which is somewhat different from the line of the theoretical quantiles. This indicates that the quantiles of the simulated paths come from a normal distribution, but one with a different variance than the asymptotic one. It is no surprise that this occurs for the lowest frequency and the smallest time interval, as for low frequencies one observes – regardless of the fineness of the sampling – the fewest full cycles over a time interval of fixed length. For this combination of time horizon and frequency we see only one full cycle.

Turning to Figure 2, we first notice that the fit in the tails improves again clearly with increasing $(T, 1/h_{\max})$. Especially, for the highest $(T, 1/h_{\max})$ one sees that the fit in the tails is a bit worse now for a driving Variance Gamma process compared with the driving Brownian motion in Figure 1. Of course, now the simulated values are indeed only asymptotically following a Gaussian distribution. Looking at the different non-zero frequencies one again sees that the fit improves for the higher frequencies. Most notably for the lowest frequency one sees for the smallest $T = 10$ again that the points do seem to lie on a straight line in the normal QQ-plot, but one with a different slope than for the theoretical quantiles. Hence, the variance is clearly different from the asymptotic one. Obviously, this effect is now more pronounced than in the case of the driving Brownian motion.

Moving on to the case of the driving process being a two-sided Poisson process in Figure 3 we first of all note that again the fit in particular in the tails clearly improves with increasing $(T, 1/h_{\max})$. For the highest $(T, 1/h_{\max})$ the simulated and theoretical asymptotic quantiles agree again extremely well. Again it is certainly a bit worse than in the case of a driving Brownian motion, but it seems to be very similar to the Variance Gamma case, although maybe for frequency 0 the agreement of the quantiles is slightly worse. Turning to the behaviour across non-zero frequencies, we see again that the quantiles are closer for higher frequencies and that for the smallest non-zero frequency and time horizon the empirical

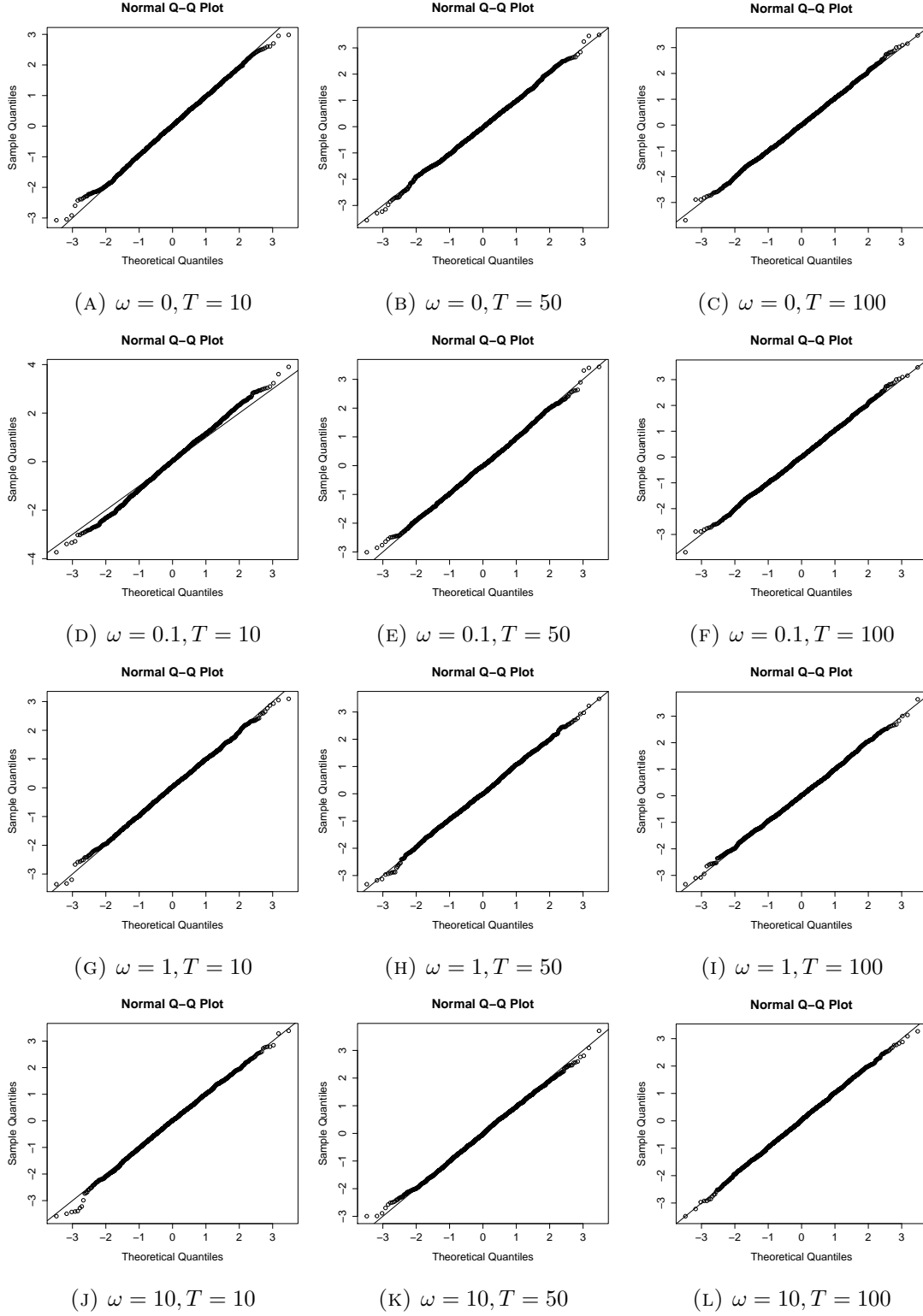


FIGURE 1. Normal QQ plots for the real part of the truncated Fourier transform of the Ornstein-Uhlenbeck type process driven by standard Brownian Motion for the frequencies 0, 0.1, 1, 10 (rows) and time horizons/maximum non-equidistant grid sizes 10/0.1, 50/0.05, 100/0.01 (columns). The theoretical quantiles are coming from the (limiting) law described in Theorem 3.15.

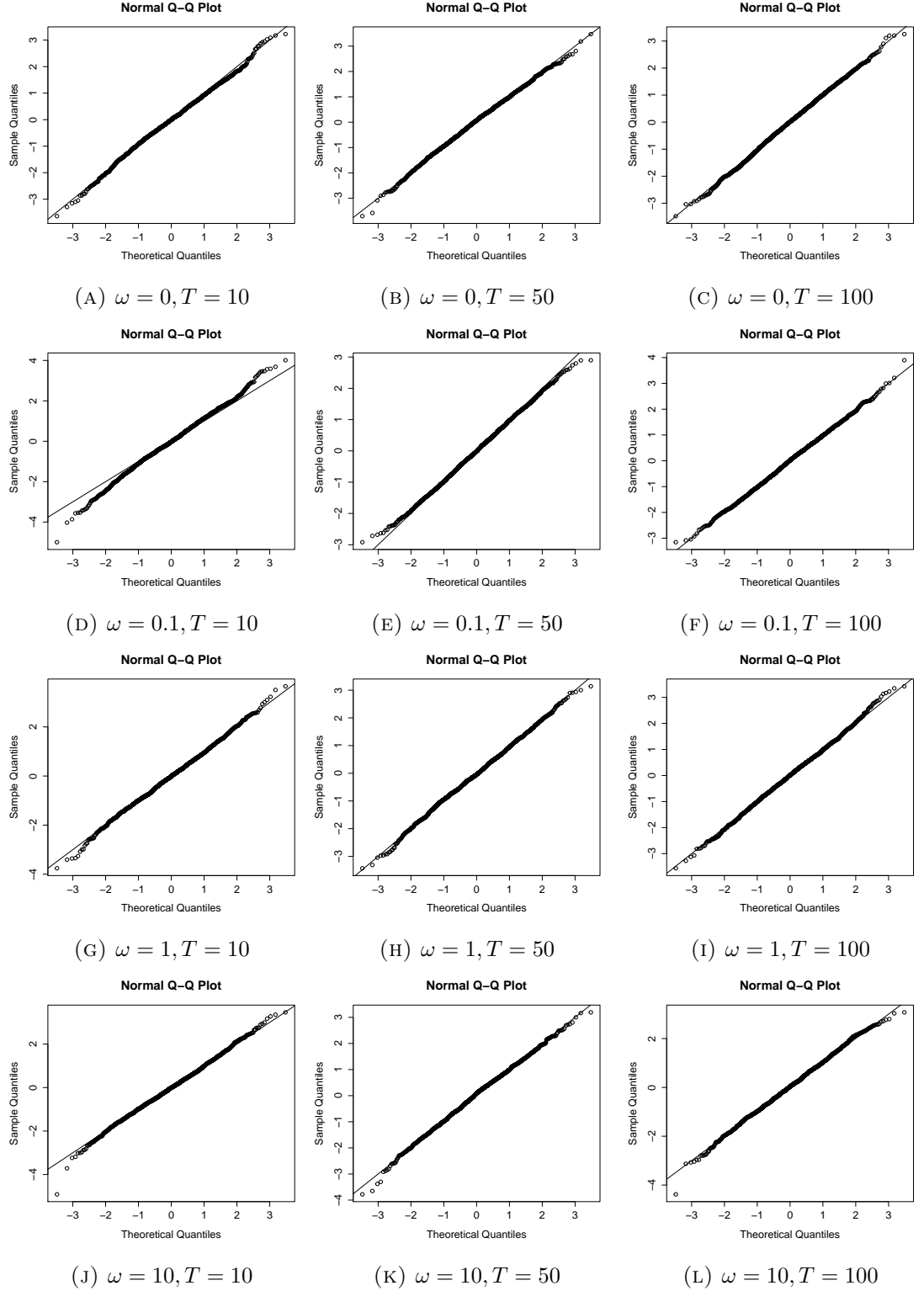


FIGURE 2. Normal QQ plots for the real part of the truncated Fourier transform of the Ornstein-Uhlenbeck type process driven by a Variance Gamma process for the frequencies 0, 0.1, 1, 10 (rows) and time horizons/maximum non-equidistant grid sizes 10/0.1, 50/0.05, 100/0.01 (columns). The theoretical quantiles are coming from the (limiting) law described in Theorem 3.15.

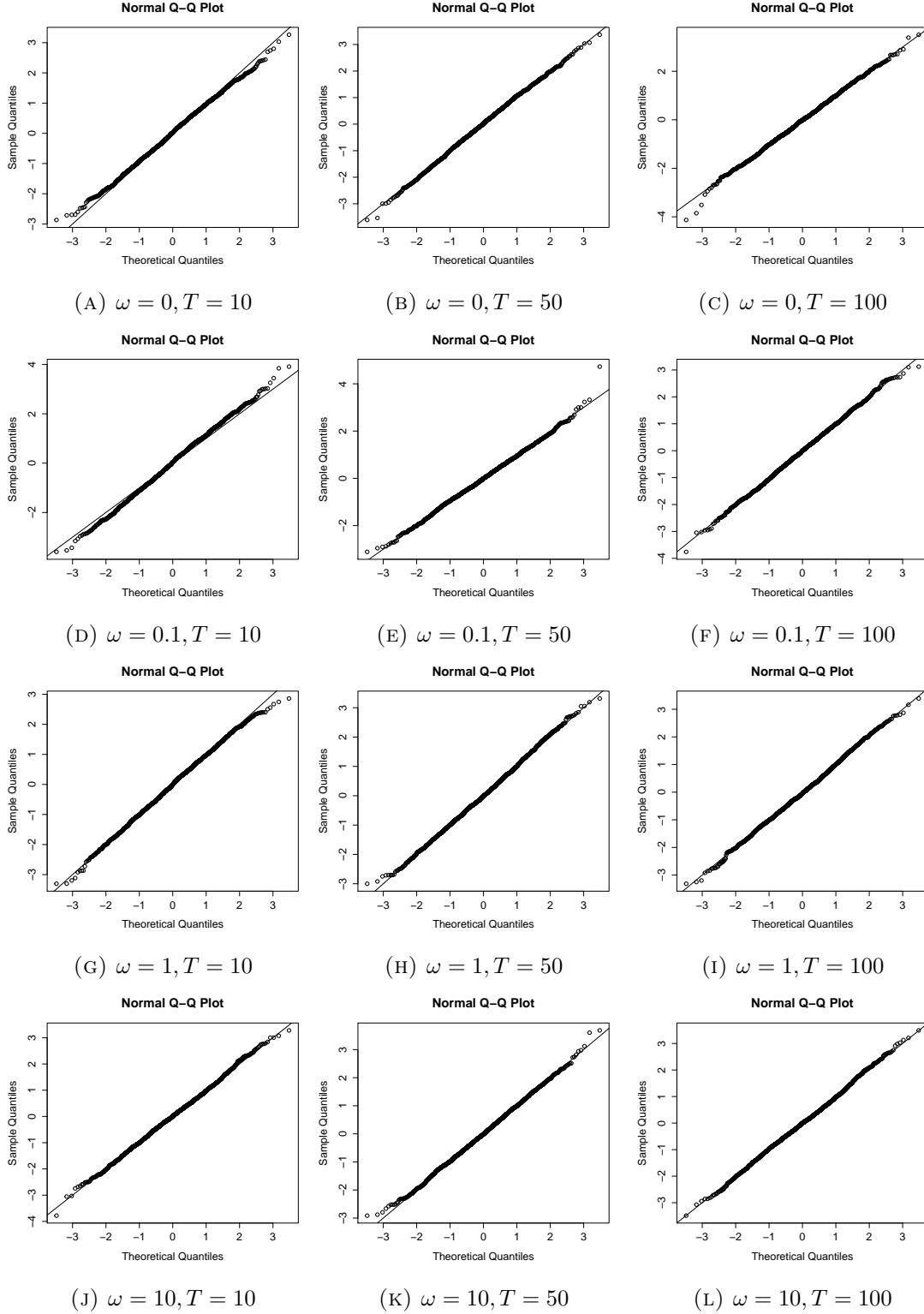


FIGURE 3. Normal QQ plots for the real part of the truncated Fourier transform of the Ornstein-Uhlenbeck type process driven by a two-sided Poisson process for the frequencies 0, 0.1, 1, 10 (rows) and time horizons/maximum non-equidistant grid sizes 10/0.1, 50/0.05, 100/0.01 (columns). The theoretical quantiles are coming from the (limiting) law described in Theorem 3.15.

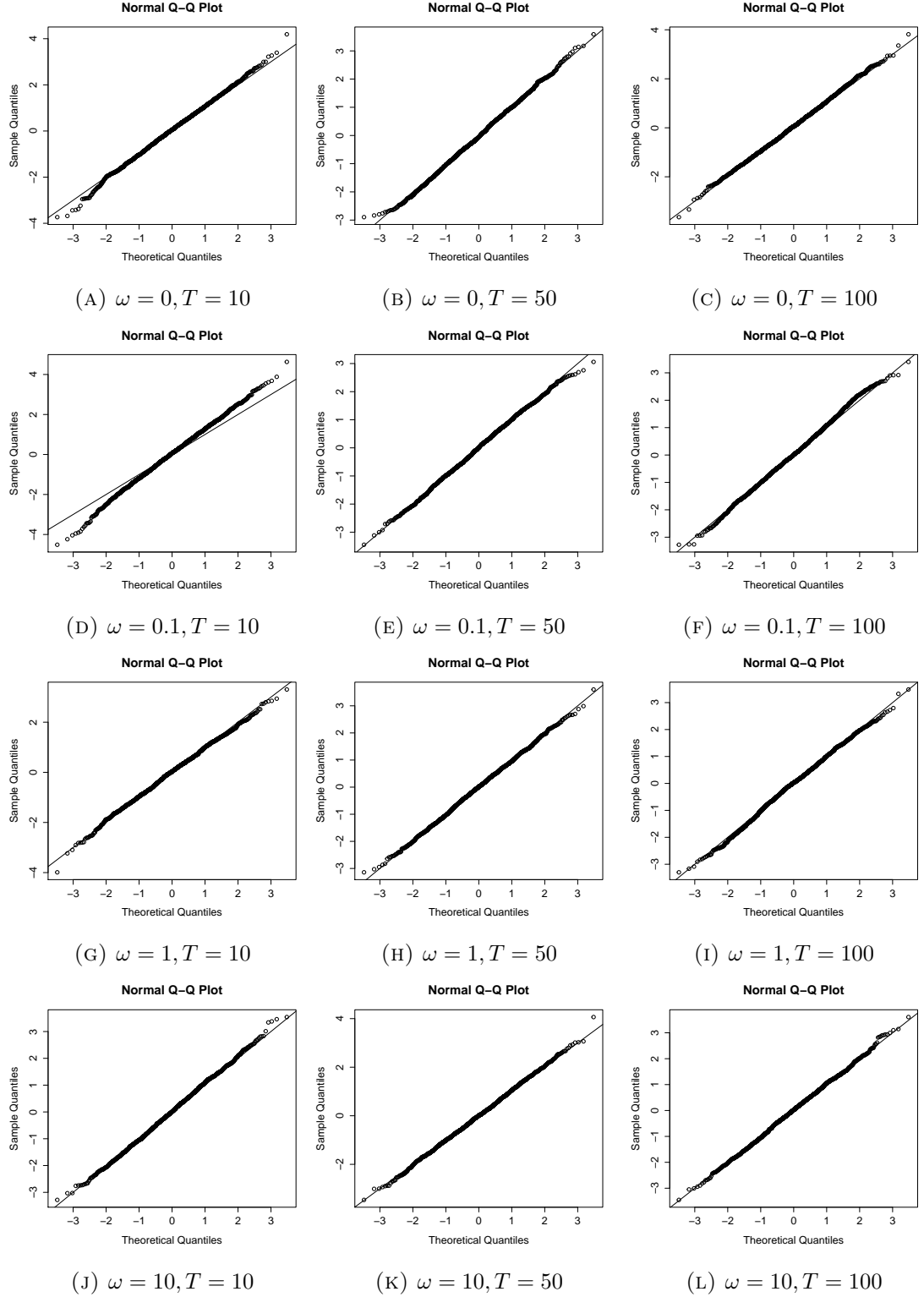


FIGURE 4. Normal QQ plots for the real part of the truncated Fourier transform of the simulated CARMA(2,1) processes driven by standard Brownian Motion for the frequencies 0, 0.1, 1, 10 (rows) and time horizons/maximum non-equidistant grid sizes 10/0.1, 50/0.05, 100/0.01 (columns). The theoretical quantiles are coming from the (limiting) law described in Theorem 3.15.

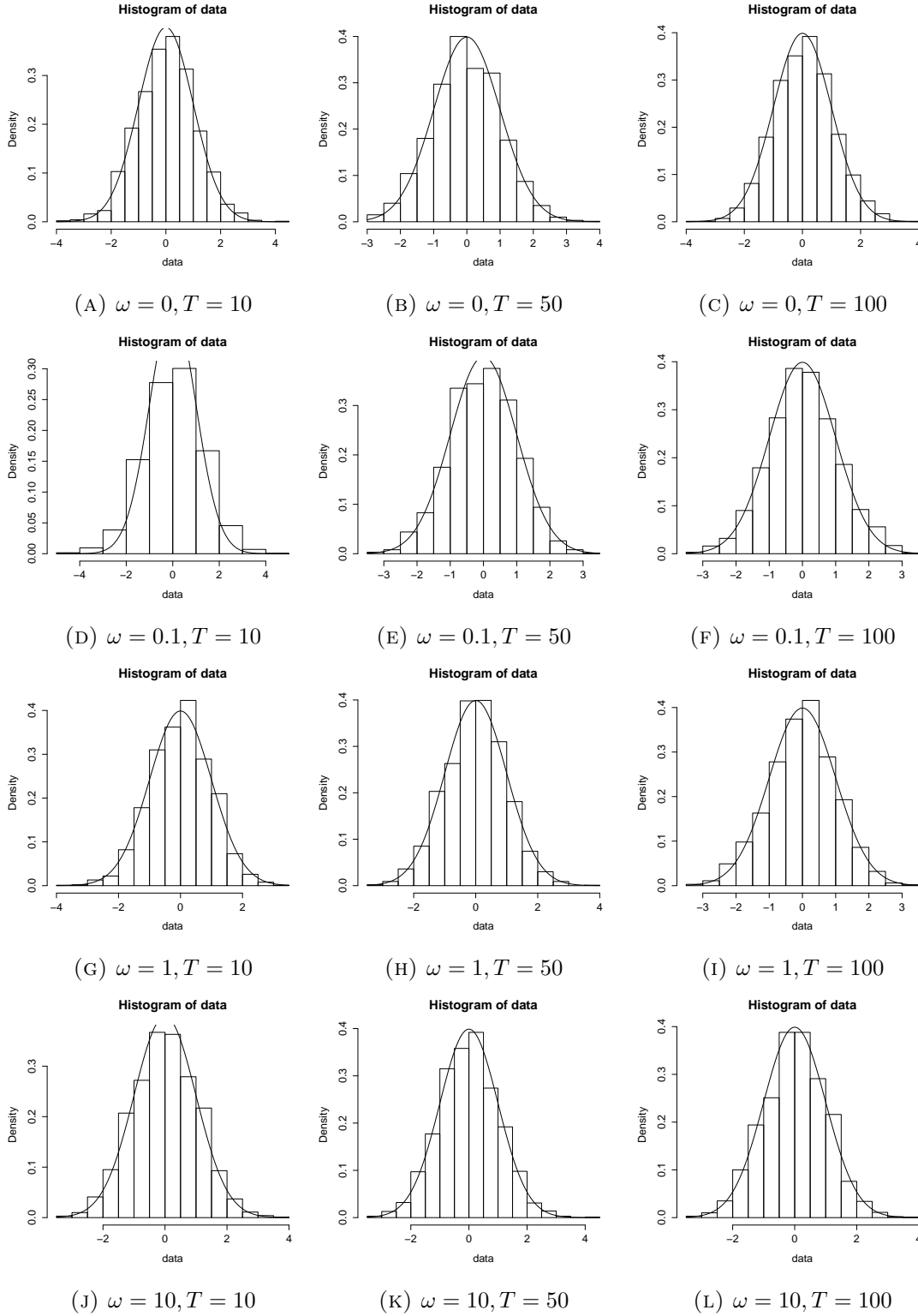


FIGURE 5. Histograms and limiting density for the real part of the truncated Fourier transform of the simulated CARMA(2,1) processes driven by standard Brownian Motion for the frequencies 0, 0.1, 1, 10 (rows) and time horizons/maximum non-equidistant grid sizes 10/0.1, 50/0.05, 100/0.01 (columns)

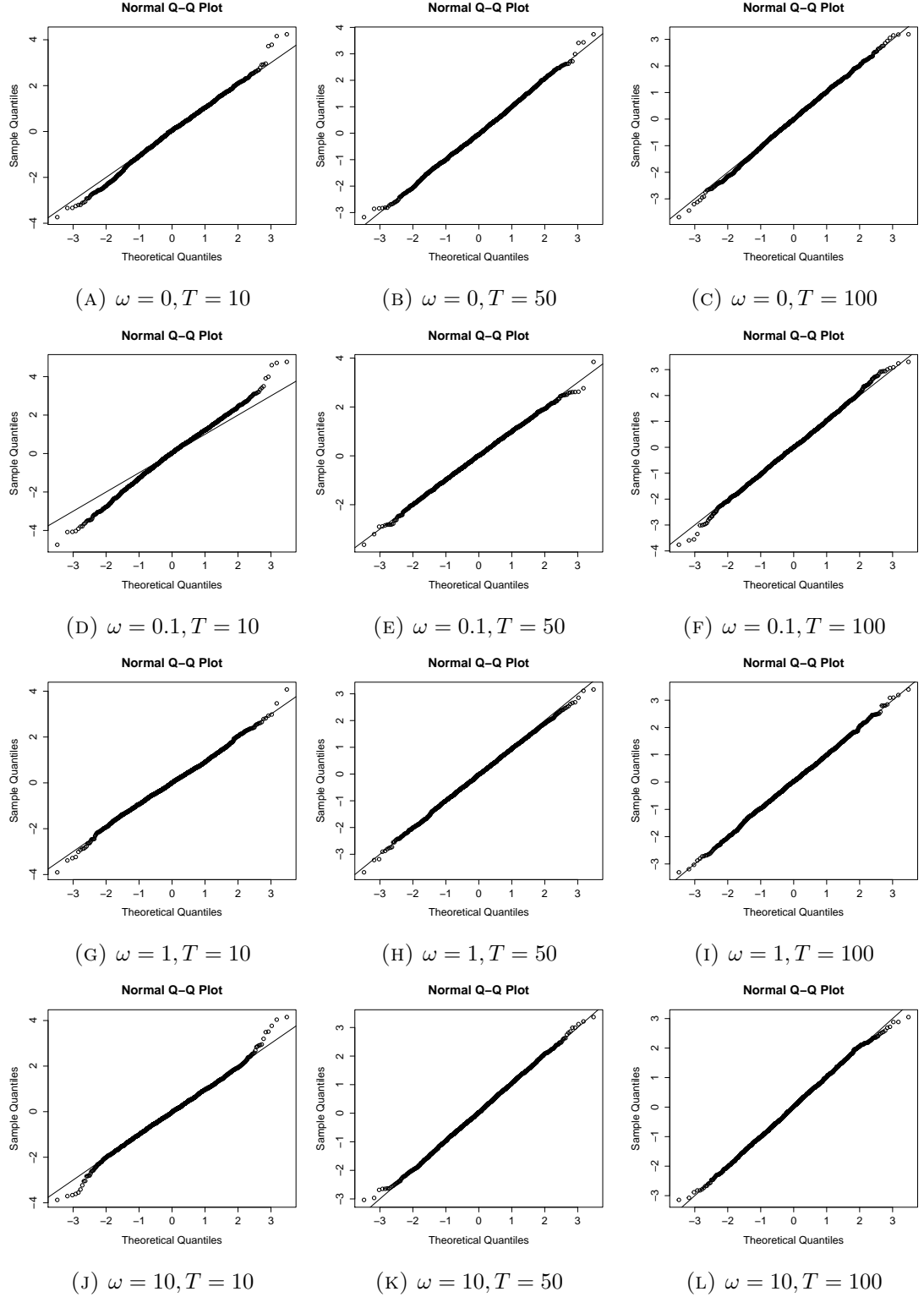


FIGURE 6. Normal QQ plots for the real part of the truncated Fourier transform of the simulated CARMA(2,1) processes driven by a Variance Gamma process for the frequencies 0, 0.1, 1, 10 (rows) and time horizons/maximum non-equidistant grid sizes 10/0.1, 50/0.05, 100/0.01 (columns). The theoretical quantiles are coming from the (limiting) law described in Theorem 3.15.

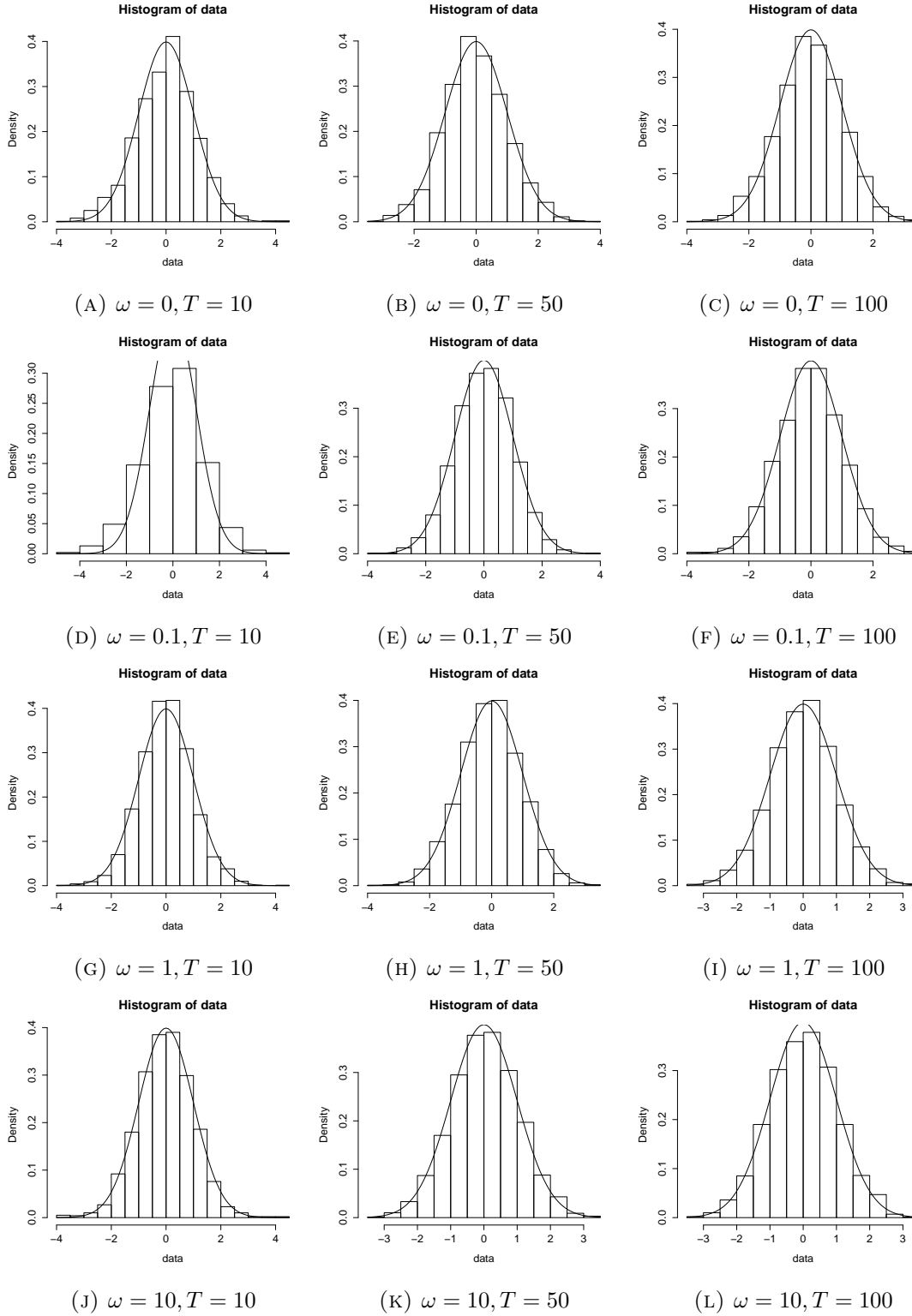


FIGURE 7. Histograms and limiting density for the real part of the truncated Fourier transform of the simulated CARMA(2,1) processes driven by a Variance Gamma process for the frequencies 0, 0.1, 1, 10 (rows) and time horizons/maximum non-equidistant grid sizes 10/0.1, 50/0.05, 100/0.01 (columns)

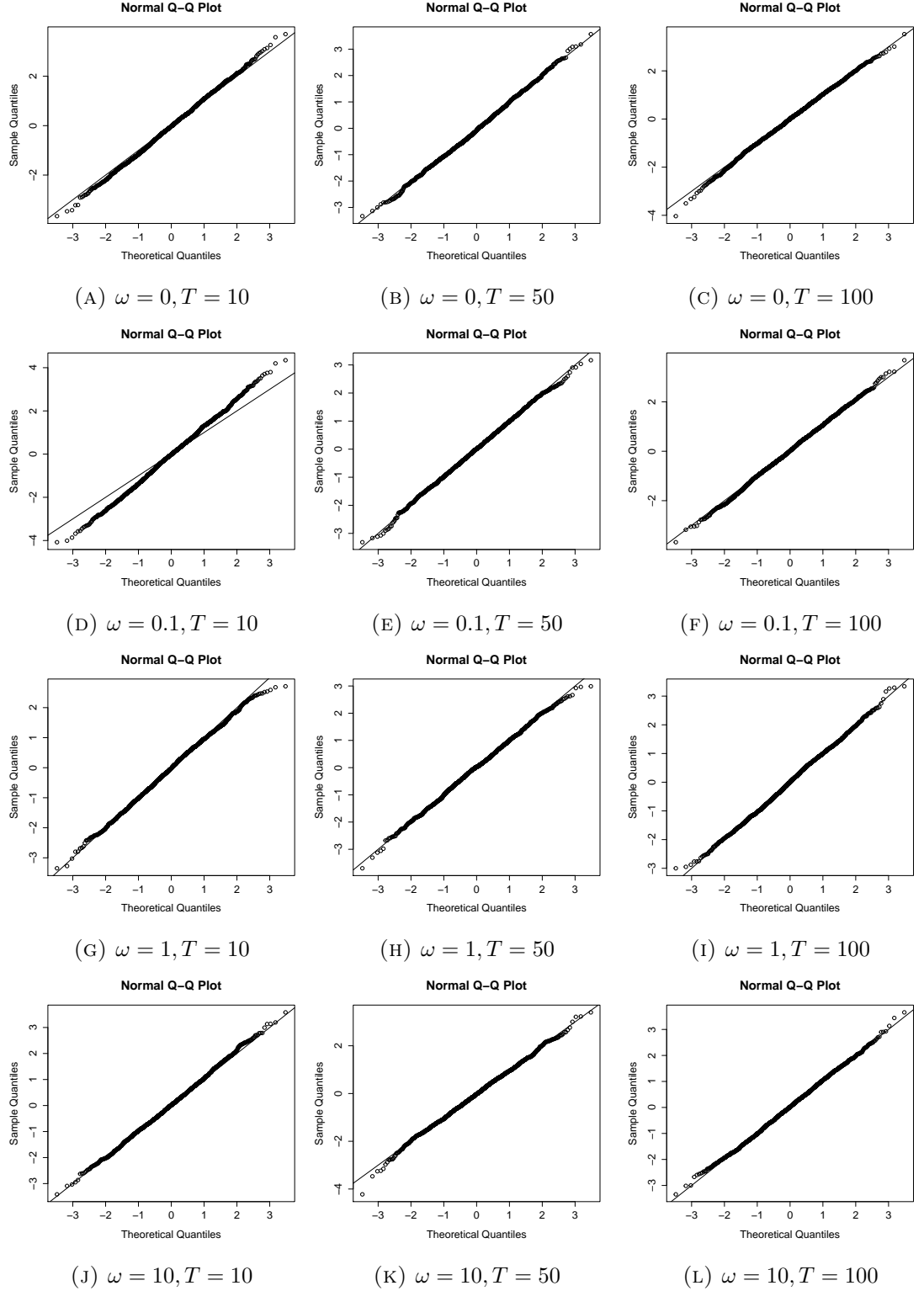


FIGURE 8. Normal QQ plots for the real part of the truncated Fourier transform of the simulated CARMA(2,1) processes driven by a two sided Poisson process for the frequencies 0,0.1,1,10 (rows) and time horizons/maximum non-equidistant grid sizes 10/0.1, 50/0.05, 100/0.01 (columns). The theoretical quantiles are coming from the (limiting) law described in Theorem 3.15.

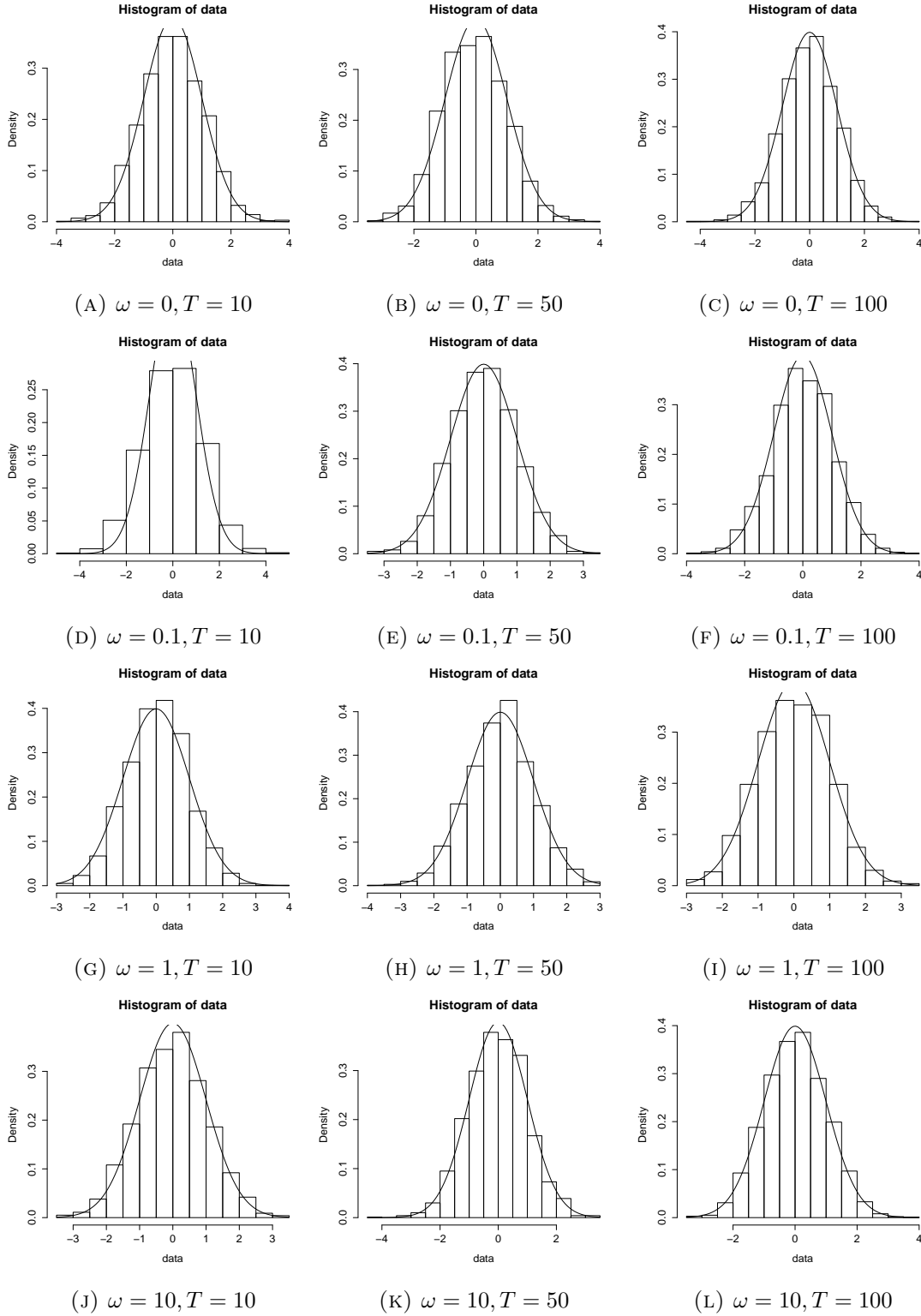


FIGURE 9. Histograms and limiting density for the real part of the truncated Fourier transform of the simulated CARMA(2,1) processes driven by a two-sided Poisson process for the frequencies 0, 0.1, 1, 10 (rows) and time horizons/maximum non-equidistant grid sizes 10/0.1, 50/0.05, 100/0.01 (columns)

quantiles seem to be in line with a normal distribution with a somewhat different variance compared to the asymptotic one. The size of this effect seems to be rather similar to the Variance Gamma case. Interestingly, also at frequency 0 the QQ-plot seems to indicate for $T = 10$ that the empirical quantiles are close to the ones of a normal distribution with a slightly different variance than the asymptotic one.

To summarize the simulation study in the CAR(1)/OU-type case we can clearly conclude that the asymptotic distribution result approximates the finite-sample distribution of the trapezoidal approximation of the truncated Fourier transform in our simulations very well and that the convergence to the asymptotic distribution is fast. For small frequencies, especially when one has about one full cycle or less over the time horizon considered, one has to be careful, as then the distribution tends to be somewhat different from the asymptotic one for good reasons. This effect seems to be more pronounced when one considers a Lévy process with jumps compared to a Brownian motion. In general the quality of the approximation of the simulated quantiles by the asymptotic ones is somewhat better in the case of a Brownian motion than in a pure jump process. Comparing the driving jump processes, the finite activity rather discrete two-sided Poisson process with the infinite activity Variance Gamma process, we do not see any significant differences. It should be noted that both jump processes are, however, light-tailed in the sense that they have exponential moments. It would not be surprising if this picture changes when considering a really heavily tailed driving Lévy process. Note that our theoretical results are valid also in rather heavily-tailed cases. For the asymptotic normality of the (trapezoidal approximation of the) truncated Fourier transform we only needed finite second moments.

Turning to the simulations of CARMA(2,1) processes, most of the findings of the CAR(1)/OU case remain valid, so we only point out the differences. In the case of a driving Brownian motion, depicted in Figure 4, the only difference seems to be that for $T = 10$ and $\omega = 0.1$ the empirical quantiles are now appearing to lie on a line farther away from the theoretical quantiles which implies that in the CARMA(2,1) case the variance in the simulations is clearly farther away from the asymptotic one than in the OU case. The same applies for the Variance Gamma case of Figure 6 and the two-sided Poisson case of Figure 6. On top of the QQ plots we now also provide histograms in Figures 5, 7 and 9, respectively, together with plots of the limiting normal density. To us it seems very hard to see the convergence to normality with increasing T in the histograms, which reflects the fact that it is essentially the tails which need to converge and they are much clearer visible in the QQ plots than in histograms. It is also not easy to see in them that for $\omega = 0.1$, $T = 10$ the variance of the simulated values is different from the asymptotic theoretical one. The only thing one notices is that for $\omega = 0.1$, $T = 10$ the histogram routine of R tends to use very different bins than in all the other cases. Note that all histograms were obtained using the default parameters of the `hist` function in R, so the binning was done by the standard automatic selection to give “nice” histograms. Hence, from our simulations of CARMA(2,1) processes we can conclude that the orders of the CARMA processes and the particular autoregressive and moving average parameters appear not to really matter for the (qualitative) behaviour of the (trapezoidal approximation of the) truncated Fourier transform.

5. CONCLUSION AND OUTLOOK

We have obtained an asymptotic normality result for the (trapezoidal approximation of the) truncated Fourier transform under essentially minimal assumptions (i.e. second moments) and seen via a simulation study that this result approximates the finite sample

behaviour very well, unless the frequency is too low compared to the length of the considered time interval. This suggests clearly that it should be very promising to develop statistical inference techniques for non-equidistantly sampled CARMA processes by considering continuous observation techniques and using numerical approximation schemes to compute the quantities of interest based on the observed non-equidistant data. The appropriate set-up to get convergence and asymptotic distribution results is to send the time horizon to infinity and to send at the same time the maximum distance of observation time points to zero.

Based on our results in this paper it seems natural to locally smooth the trapezoidal approximation of the truncated Fourier transform to get consistent estimators of the spectral density and to use it in a Whittle type estimator for the AR and MA parameters. Considering this is beyond the scope of the present paper.

ACKNOWLEDGEMENTS

The authors gratefully acknowledge the support of Deutsche Forschungsgemeinschaft (DFG) by research grant STE 2005/1-2.

The authors would like to cordially thank Włodzimierz Fechner for careful reading of the manuscript and his helpful remarks.

REFERENCES

- [1] David Applebaum, *Lévy processes and stochastic calculus*, Second Edition, Cambridge University Press, Cambridge, 2009.
- [2] Patrick Billingsley, *Probability and measure*, Third, Wiley Series in Probability and Mathematical Statistics, John Wiley & Sons, Inc., New York, 1995.
- [3] Peter J. Brockwell, *Lévy-driven CARMA processes*, Ann. Inst. Statist. Math. **53** (2001), no. 96-120, 113–124.
- [4] ———, *Continuous-time ARMA processes*, in: Handbook of Statistics, Eds.: D.N. Shanbhag, C.R. Rao, vol. 19, North-Holland, Amsterdam, 2001.
- [5] ———, *Representations of continuous-time ARMA processes*, J. Appl. Probab **41A** (2004), 375–382.
- [6] ———, *Lévy driven continuous-time ARMA processes*, in: Handbook of financial time series, Eds.: T.G. Andersen, R.A. Davis, J.-P. Kreiss and T. Mikosch, Heidelberg: Springer, 2009.
- [7] Peter J. Brockwell and Richard A. Davis, *Time series: theory and methods*, Springer, New York, 2006. Reprint of the 2nd (1991) edition.
- [8] Peter J. and Davis Brockwell Richard A. and Yang, *Estimation for non-negative Lévy-driven CARMA processes*, J. Bus. Econom. Statist. **29** (2011), no. 2, 250–259.
- [9] Peter J. Brockwell and Alexander Lindner, *Existence and uniqueness of stationary Lévy-driven CARMA processes*, Stochastic Process. Appl. **119** (2009), no. 8, 2660–2681.
- [10] Peter J. Brockwell and Eckhard Schlemm, *Parametric estimation of the driving Lévy process of multivariate CARMA processes from discrete observations*, J. Multivariate Anal. **115** (2013), 217–251.
- [11] J. L. Doob, *The elementary Gaussian processes*, Ann. Math. Statistics **15** (1944), 229–282.
- [12] V. Fasen, *Statistical inference of spectral estimation for continuous-time MA processes with finite second moments*, Math. Methods Statist. **22** (2013), no. 4, 283–309.
- [13] Vicky Fasen and Florian Fuchs, *Spectral estimates for high-frequency sampled continuous-time autoregressive moving average processes*, J. Time Series Anal. **34** (2013), no. 5, 532–551.
- [14] ———, *On the limit behavior of the periodogram of high-frequency sampled stable CARMA processes*, Stochastic Process. Appl. **123** (2013), no. 1, 229–273.
- [15] Jonas Gillberg, *Frequency Domain Identification of Continuous-Time Systems: Reconstruction and Robustness*, Linköping Studies in Science and Technology. Dissertations **1031** (2006).
- [16] Keh-Shin Lii and Elias Masry, *Model fitting for continuous-time stationary processes from discrete-time data*, J. Multivariate Anal. **41** (1992), no. 1, 56–79.
- [17] ———, *Spectral estimation of continuous-time stationary processes from random sampling*, Stochastic Process. Appl. **52** (1994), no. 1, 39–64.

- [18] Dilip B. Madan, Peter P. Carr, and Eric C. Chang, *The Variance Gamma Process and Option Pricing*, European Finance Review **2** (1998), 79–105.
- [19] Tina Marquardt and Robert Stelzer, *Multivariate CARMA processes*, Stochastic Process. Appl. **117** (2007), no. 1, 96–120.
- [20] Philip E. Protter, *Stochastic integration and differential equations*, 2nd edn., Springer-Verlag, Berlin, 2004.
- [21] Eckhard Schlemm and Robert Stelzer, *Multivariate CARMA processes, continuous-time state space models and complete regularity of the innovations of the sampled processes*, Bernoulli **18** (2012), no. 1, 46–63.
- [22] Erik Talvila and Matthew Wiersma, *Simple derivation of basic quadrature formulas*, Atl. Electron. J. Math. **5** (2012), no. 1, 47–59.
- [23] Mark Veraar, *The stochastic Fubini theorem revisited*, Stochastics **84** (2012), no. 4, 543–551.

¹ INSTITUTE OF MATHEMATICS, UNIVERSITY OF SILESIA, BANKOWA 14, 40-007 KATOWICE, POLAND,

² INSTITUTE OF MATHEMATICAL FINANCE, ULM UNIVERSITY, HELMHOLTZSTRASSE 18, 89069 ULM, GERMANY

E-mail address: `zfechner@gmail.com`, `robert.stelzer@uni-ulm.de`